Review
doi.org/10.1002/ansa.202100007
Chemistry Europe
European Chemical Societies Publishing

Received: 21 January 2021
Accepted: 1 March 2021

# Advances in ultra-high-pressure and multi-dimensional liquid chromatography instrumentation and workflows

**Jelle De Vos**[1] | **Dwight Stoll**[2] | **Stephan Buckenmaier**[3] | **Sebastiaan Eeltink**[1] | **James P. Grinias**[4]

[1] Department of Chemical Engineering, Vrije Universiteit Brussel (VUB), Brussels, Belgium

[2] Department of Chemistry, Gustavus Aldophus College, Saint Peter, Minnesota, USA

[3] Agilent Technologies, Research and Development, Waldbronn, Germany

[4] Department of Chemistry and Biochemistry, Rowan University, Glassboro, New Jersey, USA

**Correspondence**
Jelle De Vos, Department of Chemical Engineering, Vrije Universiteit Brussel (VUB), Brussels, Belgium
Email: Jelle.De.Vos@vub.be

**Funding information**
Chemical Measurement and Imaging Program in the National Science Foundation Division of Chemistry, Grant/Award Number: CHE-2045023; Research Foundation Flanders (FWO), Grant/Award Numbers: research project G033018N, senior postdoctoral fellowship 12J6520N; Research Foundation Flanders and the Fonds de la Recherche Scientifique (FWO-FRNS), Grant/Award Number: Excellence of Science grant (30897864)

## Abstract

The present contribution discusses recent advances in ultra-high-pressure liquid chromatography (UHPLC) and multi-dimensional liquid chromatography (MDLC) technology. First, new developments in UHPLC column technology and system design are highlighted. The latter includes a description of a novel injector concept enabling method speed-up, emerging detectors, and instrument diagnostics approaches. Next, online MDLC workflows are reviewed and advances in modulation technology are highlighted. Finally, key applications published in 2020 are reviewed.

**KEYWORDS**
UHPLC, two-dimensional liquid chromatography, 2D-LC, spatial three-dimensional liquid chromatography

## 1 | RESOLVING POWER IN LIQUID CHROMATOGRAPHY

Increasing the resolving power of the separation method has always been at the forefront of scientific developments in analytical separation science. Traditionally, it is expressed in terms of the theoretical plate number ($N$), which increases with the square power of analysis time. The interpretation of chromatographic performance limits using a graphical representation expressed by the achievable plate number and required analysis time, was pioneered by Giddings.[1,2] Such a plot incorporated column characteristics, as both van Deemter parameters and column permeability are taken into account, and considers operation conditions and system characteristics, such as mobile-phase viscosity and the maximum system pressure available. This concept was further refined by Poppe,[3] who proposed to plot the plate time, defined as $t_0/N$ as a function of $N$. Desmet and co-workers have expanded the theoretical framework and introduced different kinetic plot representations for separations conducted in isocratic and gradient LC mode. More recently kinetic gain factors were defined, allowing users to predict and experimentally determine the gain in either time or efficiency that can be obtained when changing LC instruments[4,5]. These plots also provide valuable insights into possible optimization routes to be

doi.org/10.1002/ansa.202100007


considered with respect to column technology and instrumentation, as one can, for example, consider the effect of the maximum operating pressure on efficiency and resulting analysis time. The improvements in kinetic gain factors when moving from conventional HPLC to 1500 bar UHPLC operating conditions were experimentally demonstrated by De Vos *et al*.[6] For isocratic separations ($N \leq 80\,000$), the highest peak-production rate was achieved by selecting columns packed with 1.5 µm core-shell particles operated at 1500 bar, over 2.6 µm particles. When these sub-2 µm particles were used in gradient mode, a kinetic time-gain factor of 13 was established for the separation of a complex mixture of waste-water pollutants, compared to conventional HPLC conditions at 500 bar. Recently, Broeckhoven *et al*. discussed the potential gain in performance when increasing the pressure rating further to 3000 bar.[7] The authors reported a two-fold reduction in terms of speed of analysis can be attained at those operating pressures with respect to a modern UHPLC system operating at 1500 bar. In order to realize this, a paradigm shift needs to be realized in the development of well-packed and pressure stable narrow bore (1 mm i.d.) column housing packed with sub-2 µm particles and instruments that feature significantly reduced extra-column band broadening contributions. Deformation of the column hardware and particles can affect the stability of the packed bed and column porosity. The change in physicochemical factors, that is, increase in melting point and increased viscosity of solvents, can also impede the use of extreme pressures in LC.

Multidimensional techniques offer great potential to improve the resolving power, since the separation performance of the LC system increases approximately with $n^i$ (where $n$ is the number of resolvable peaks and $i$ the dimensionality).[8] This fundamental law of dimensionality results in a massive challenge, both in instrument design and stationary phase development, to provide robust technology for multidimensional separations. Clearly, this can only be realized by building on the advanced developments of one-dimensional LC technology. The foundations for HPLC instrumentation are well developed, aided by the recent introduction of ultra-high pressure LC technology.[9–12] This gives researchers the means to build a set-up for multidimensional separations, or buy a commercially available instrument, lowering the barrier to entry to a growing number of specialists. The progress and future developments will be dictated by the choice of the instrumentation, advances in column technology, the development of effective ways of combining separation modes (*ie*, modulation technology), and the progress in data-processing techniques.

## 2 | UHPLC TECHNOLOGY

The first demonstrations of what is now referred to as ultra-high pressure liquid chromatography (UHPLC) were made in the late 1960s, when separations were conducted in the 3500-4000 bar range.[13–19] The current approaches to UHPLC were more firmly established in the mid-1990s when the Jorgenson group demonstrated capillary UHPLC separations performed up to 7000 bar.[20–23] Based on the high chromatographic efficiencies that were obtained using long capillary columns packed with sub-2 µm particles, LC instrument manufacturers recognized the potential for commercial LCs with higher pressure limits. The first commercial UHPLC instrument was released in 2004, with an upper pressure limit of 1000 bar that more than doubled the industry HPLC standard of 400 bar that had existed for over 30 years.[11,24] Since that time, a variety of UHPLC instruments from various manufacturers have been introduced, with pressure limits of commercial instrumentation now as high as 1500 bar.[9] An overview of recent developments in UHPLC instrument configurations is provided in Table 1.

### 2.1 | Column design

The current state-of-the-art UHPLC column technology are 2.1 mm i.d. column formats packed with sub-2-micron particle technology. Whereas 4.6 mm i.d. columns had been the gold standard for many decades, the move to 2.1 mm i.d. column formats was mandatory to address effects of viscous heating when operating at ultra-high pressure conditions. When forcing the flow through the interstitial voids of the column packing, a significant temperature increase is observed towards the column outlet, which consequently affects the retention properties.[25] As heat is dissipated via the column wall, a radial temperature gradient is formed and the resulting parabolic flow profile will have a detrimental impact on chromatographic efficiency.[26] By reducing the cross section of the column to 2.1. mm i.d. and operating with an optimized column-oven configuration, the impact of frictional heating on the chromatographic separation is markedly lower than what would be expected for 4.6 mm i.d. columns running at similar linear velocities, which corresponds to a nearly five-fold increase in flow rate. Significant advances have also been realized in the column technology development with respect to particle size and type.[12] Decreased particle diameter leads to lower plate height values as the eddy-dispersion contribution (*A*-term) is proportional to particle diameter and the resistance to mass transfers (*C*-term) decreases proportional to the square of the particle diameter.[27] Over one decade ago, core-shell particles were re-introduced as an attractive column format for UHPLC applications.[28] These particles feature a small porous layer surrounding an impervious solid core, which also displays different meso-porous characteristics compared to fully porous particles. As a result, core-shell particles have reduced *B*-term band broadening of up to 40%, which, together with lower *A*- (up to 40%) and *C*-term (typically around 50%, but analyte dependent) contributions give rise to an improved kinetic performance.[28–30] While the mass loadability and retention capacity of core-shell particles is somewhat lower than that of fully porous particles, the loss is relatively limited as the porous layer typically makes up about 70% of the total volume of the particle.[28] Classical core-shell particle technology is based on a silica precursor and the different methods of preparation have been described in a review paper by Tanaka and McCalley.[31] Recently, Lesko *et al*. investigated the nature and magnitude of temperature gradients in UHPLC, utilizing columns packed with classical silica-based fully porous and core-shell particles. Furthermore, these results were compared to that of columns packed with 3.6 µm core-shell particles comprising a graphite core

**TABLE 1** Overview of recent UHPLC and multidimensional LC platforms. Manufacturers of the platforms are: Agilent Technologies (Infinity II, RapidFire, StreamSelect), Sciex (MPX), Shimadzu (i-Series Plus, Nexera), ThermoFisher Scientific (CL Series, Vanquish), Waters Corporation (ACQUITY)

| Characteristic Property | Relevant Commercial Instrument Platforms |
|---|---|
| High pressure limit with reduced system volume for maximum performance | ACQUITY UPLC I-Class PLUS System<br>Vanquish Horizon UHPLC System<br>1290 Infinity II LC System<br>Nexera X3 |
| Medium pressure limit designed to bridge HPLC and UHPLC methods | ACQUITY Arc System<br>Vanquish Core HPLC System<br>1260 Infinity II Prime LC System<br>Nexera XR |
| Simplified 2D-LC platform | ACQUITY Arc Multi-Dimensional Liquid Chromatography System<br>ACQUITY UPLC M-Class System with 2D Technology<br>1290 Infinity II 2D-LC System<br>Vanquish Online 2D-LC Systems<br>Nexera-e |
| Smart user diagnostic feedback (mobile phase usage, pressure spikes, etc.) | Vanquish Core HPLC System<br>Nexera series (X3, XS, XR) |
| High sample throughput platform, primarily for MS detection | Vanquish Duo UHPLC System (Transcend Duo LX-2 workflow)<br>StreamSelect LC/MS System<br>RapidFire 400<br>MPX 2.0 High Throughput System |
| Systems designed for specific applications | Vanquish MD HPLC (*clinical diagnostics*)<br>ACQUITY Advanced Polymer Chromatography System (*polymer characterization*)<br>ACQUITY UPLC M-Class System with HDX Technology (*protein conformation*)<br>ACQUITY UPLC I-Class IVD System (*clinical diagnostics*)<br>1260 Infinity II Amino Acid Analysis System (*amino acids*)<br>1260 Infinity II GPC/SEC System (*polymer characterization*)<br>Clinical Edition TQ LC/MS System (*clinical diagnostics*)<br>Nexera Post-Column Analysis Systems (*amino acids & reducing sugars*)<br>Nexera GPC system (*polymer characterization*)<br>CL Series (*clinical diagnostics*)<br>i-Series Plus Analyzers (*cannabis potency, hemp, & bioethanol*) |
| Bio-inert flow paths | 1260 Infinity II Bio-Inert LC System<br>1290 Infinity II Bio LC System<br>ACQUITY UPLC H-Class PLUS Bio System<br>Vanquish Horizon UHPLC, Integrated Biocompatible System<br>Nexera Bio |

surrounded by a thin (0.1 µm) diamond shell.[32] When comparing the silica and diamond core-shell particulate columns it was observed that at UHPLC conditions that an axial temperature gradient still exists, but the temperature at the column outlet packed with silica-based material is higher. Applying isothermal conditions (*i.e.*, a water bath acting as column oven) the radial temperature gradient was significantly diminished using the core-shell particle column with the diamond shell structure, as the latter material is characterized by a much higher effective heat conductivity. Wouters *et al*. reported on a novel column format for ultra-high-pressure ion chromatography (UHPIC).[33] To establish a metal-free fluidic path compatible with corrosive solvents while operating at UHPIC conditions, prototype columns were developed utilizing PEEK-lined SS tubing and PEEK seats and frits, see Figure 1A. Columns were packed with 2.5 µm microporous polymer-based particles and 2.5 µm macroporous particle beads, both coated with nanobeads yielding the desired anion-exchange functionality. Because of the pressures that were generated, thermal heating effects on separation efficiency and retention were assessed. The PEEK lining acted as insulator (near-adiabatic operation) mediating the formation of a radial temperature gradient, and consequently maintaining high separation efficiencies. The axial temperature gradient across the column length when operating at ultra-high pressures led to a slight increase in retention for late eluting anions.

Recently, different studies were conducted to increase the understanding of column packing structure and its link to separation performance. An investigation on frit dispersion by Gritti and Gilar demonstrated that porous frits add to band variance by up to 0.5 $\mu L^2$, with the outlet frit being especially detrimental to peak capacity in gradient separations (50% less than theoretical calculated value).[34] Furthermore, effects of column bed heterogeneity and column end structure near the frits were assessed for 50, 100, and 150 mm long UHPLC columns packed with 1.7 µm fully porous particles and 1.6 µm core-shell particles by Zelanyanski *et al*.[35] A non-retained marker was injected and then traveled through the column for a given distance

Review
doi.org/10.1002/ansa.202100007
Chemistry Europe
European Chemical Societies Publishing

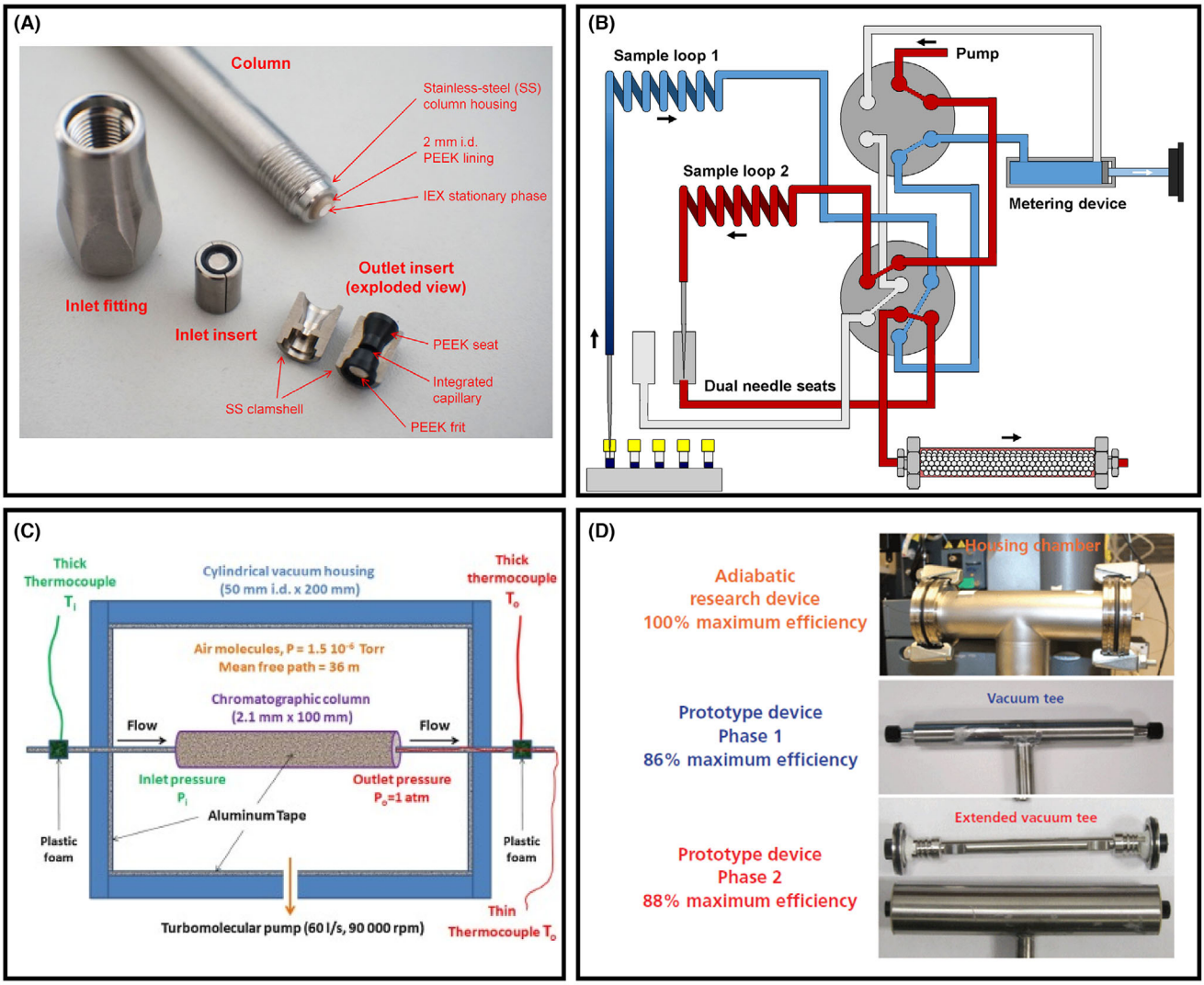


**FIGURE 1** Highlights of recent innovations in UHPLC technology considering column and instrument hardware. A, Prototype column hardware for ultra-high pressure ion chromatography. Reproduced from 33 with permission (© 2019, American Chemical Society). B, Schematic representation of a duo injector, that uses an additional valve to incorporate two flow paths (highlighted in red and blue) in a single module to realize parallel injection and reduce the total cycle time. C, Overview of the experimental set-up used to create a high-vacuum column housing that uses a turbomolecular pump to achieve adiabatic conditions. Reproduced from 79 with permission (© 2016, Elsevier B.V.). D, The actual experimental setup, that is shown schematically in Figure 1C, and prototype devices that have a small-volume column housing chamber to improve user-friendliness for routine analysis. Reproduced from 80 with permission (© 2018, MJH Life Sciences™ and Chromatography Online)

before the flow was reversed in order to estimate local plate-height values. It was concluded that column length is an influencing factor on the column packing procedure as short columns were packed more homogenously axially and the local plate height increased with column length. The flow reversal also causes a peak compression effect, which is more pronounced in biomolecules than it is in small molecules.[36] De Vos *et al.* investigated particle and bed integrity of SEC columns packed with 1.7 µm fully porous particles at pressure up to 1000 bar using 30 mm short columns to maximize the pressure drop across particles.[37] The application of ultra-high-pressure cycles (above manufacturers recommendations) led to void formation at the column inlet and some fractured particles mainly situated at the column outlet. Interparticle porosity decreased due to void formation, likely induced by the rearrangement of the packing structure, whereas intraparticle porosity as measured with argon-adsorption experiments remained largely unaffected.

## 2.2 | UHPLC instrument configuration

As decreasing the particle and column diameter both lead to significantly smaller peak volumes, extra-column volumes induced by tubing configuration and instrument modules need to be minimized to maintain high separation efficiency.[38] While decreasing injection volume, tubing diameter, and detector flow-cell volume leads to an effective reduction in dispersion, the price to pay is the increased contribution to system operating pressure, limiting the available pressure range that can be effectively applied to the column. Zhou *et al.* assessed the effects

of tubing configuration and i.d. on separation impedance and kinetic performance limits, taking both chromatographic dispersion characteristics and pressure drop into consideration.[39] The gain in separation efficiency when decreasing tubing i.d. from 100 to 75 µm was found to contribute more to the decrease in separation impedance and the position of the kinetic performance curve than the loss in available column pressure induced by the narrower tubing.[39] Gradient-elution strategies can also be used to some extent to decrease the pre-column extra-column effects, by focusing analytes at the head of the column under the weaker solvent conditions early in the gradient program. However, gradient delay volume can still affect the chromatographic separation, and post-column dispersion in connecting tubing and the detector flow cell decreases efficiency even with this gradient focusing effect.[40] Reducing the cross section of the fluidic pathway will also induce significant pressure-induced retention shifts. When increasing the column inlet pressure from 200 to almost 1200 bar and ensuring the absence of frictional heating, an increase in retention factor of 41% for late-eluting analytes (alkylphenones) was observed when decreasing the tubing i.d. from 100 to 75 µm.[39] Extra-column band broadening can be especially detrimental for high-throughput LC separations,[41] with a low system variance contribution of 2 $\mu L^2$ decreasing the peak-production rate by over 50% when using rapid "ballistic" gradient methods with cycle times on the order of 15-30 s.[42]

The current state-of-the-art commercially available UHPLC pump technology is capable of providing up to 1250-1500 bar system pressure based on a dual-piston arrangement.[43] In modern systems, careful motor control and diagnostic feedback are used to account for solvent compression and resulting thermal effects that occur during mobile phase delivery, ensuring reproducible flow rates with minimal pressure fluctuation. The most effective techniques rely upon rapid pump strokes to minimize pressure ripple and pressure profile monitoring that tracks both pressure and temperature components on volume contraction to adjust piston speed.[9] In a series dual-piston system, a primary piston with a larger displacement volume is connected to a secondary piston that delivers solvent directly to the column. During the refill phase of the secondary piston, the primary piston can deliver a larger volume of solvent that both refills the secondary piston and maintains mobile phase flow through the column. In a parallel dual-piston system, the two pistons are equivalent and designed to move 180° out-of-phase, so that one piston is always delivering mobile phase to the column while the other is refilling. Most instruments allow for high-pressure mixing, which involves independent pumping of two components of a binary solvent system that are then mixed prior to the system injector, minimizing the gradient dwell volume.[44]

In the early era of fundamental UHPLC research, where columns were operated in the 3000-7000 bar range, separations were conducted using pneumatic amplifier constant-pressure pumps. These pumps deliver mobile phase directly from a reservoir chamber to the column, with relatively large noise peaks due to pump cycling that occur during the refill stage as the stroke volume is in the 1-2 mL range. For capillary scale analysis with flow rates in the low µL/min range, a single pump stroke suffices, and flow disruptions are not observed. However, this is not the case when these pumps are used for analytical-scale columns. To demonstrate the use of pressures up to 2600 bar with 2.1 mm i.d. columns, two pumps were coupled to enable consistent solvent delivery with a secondary pump maintaining flow during the refill phase of the primary working pump.[45] This strategy reduced the pressure fluctuation during the refill phase from 14.1% to 1.6%, which enabled long runs over 100 min using a 2.1 × 600 mm column array (four 150 mm columns coupled in series, each packed with sub-2 µm particles) at a flow rate of 0.18 mL/min. To enable gradient runs with this platform, a pre-programmed solvent gradient is loaded into a storage loop and then pushed through the column at higher pressure,[46] a strategy which has also been employed for capillary LC separations in the 2000-3000 bar range.[47–50] A major challenge with combining pressures above 2000 bar with analytical-scale flow rates is the drastic increase in viscous friction effects that is observed,[7] especially in short columns in which the axial temperature increase can be up to 60 °C.[26] Solutions like intermediate cooling between column segments in series column arrays can help alleviate some of these effects.[45,51] However, a move towards smaller column diameters to be used with these higher pressures is likely necessary, which presents its own challenges in terms of preparing high efficiency columns due to bed morphology effects that reduce performance in the 1 mm i.d. range.[52]

The experiments performed at very high pressures up to 3000 bar have been conducted by applying constant pressure operation rather than the more commonly used constant flow mode. In 2011, Broeckhoven and Verstraeten *et al.* looked at the theoretical[53] and experimental[54] aspects of both modes, specifically related to the kinetic performance limits when using gradient elution. Because the flow rate will increase as the viscosity drops throughout a typical water-acetonitrile reversed-phase gradient program, operating continuously at the instrument pressure limit ensures that the maximum flow rate is achieved throughout the entire separation. Consequently, the time gain that can be realized in constant pressure mode will be largest for gradients covering a broad gradient, and hence a large mobile phase viscosity, span. The time gain that can be realized by using constant pressure mode will be in the order of 10-30%, as the flow rate increases once the gradient program reaches conditions with high organic content that have lower viscosity.[55,56] Method repeatability and quantitative performance were similar between the two modes when using concentration-sensitive absorbance detection,[57] although mass-sensitive detectors that rely upon sample nebulization can see shifting peak signals due to changes in the flow rate throughout the run.[58] Note that method transfer or HPLC to UHPLC method speed-up is more difficult under constant pressure conditions, as the gradient delay time will vary more for different elution programs than the simple correction for gradient delay volume that is needed for constant flow methods. Moreover, at UHPLC conditions, increased viscous heating induced by the overall higher flow rate when operating in constant pressure mode may affect chromatographic performance,[59] and pressure effects on solute retention may impact chromatographic resolution.[60]

The primary injector type used in high-end UHPLC instrumentation is the flow-through needle/split-loop injector.[61,62] In this case, the

needle is an inherent part of the sample loop and is placed directly into a needle seat on the injector valve after sample is drawn into the loop, which is then injected onto the column after the valve actuates. Sample precompression prior to injection is believed to increase overall column lifetime. Split-loop injectors typically have less carryover and use less sample, but typically contribute more to chromatographic bandwidth than a fixed-loop injector. The latter configuration allows the injection of larger sample volumes. The cycle time of current injection systems limits the development of high-throughput UHPLC methods. The combination of needle movement, sample-draw and needle-wash processes limits the speed at which chromatographic injections can be performed. The fastest cycle times for these autosamplers are currently in the order of 7-11 s.[63] To overcome this bottleneck, novel well-plate autosamplers were designed integrating a dual-needle design allowing to reduce the overall cycle time by overlapped chromatographic runs and injection cycles. Alternatively, the dual-needle design has been utilized in combination with a dual gradient UHPLC and two detectors, providing separate fluidic paths to double throughput, see Figure 1B for a basic layout.[64–69]

Modern column compartments are designed to facilitate still-air and/or forced-air heating.[70] In still-air mode, designed to approach adiabatic conditions, the axial thermal gradient that forms along the column length is maximized. The forced-air mode is designed to promote isothermal conditions and increases the magnitude of the radial thermal gradient that exists between the column center and wall. In practice, both thermal gradients are observed in a system,[71] although special experimental setups can be used to more closely replicate fully adiabatic or isothermal operation.[72–74] To study these effects in real-time, thermal-imaging cameras have been applied to simultaneously monitor temperature changes across the entire column,[75–77] although thermocouples can also be used.[72] To better achieve adiabatic conditions, a quasi-adiabatic vacuum jacket (displayed in Figure 1C and D) was developed by Gritti *et al.* in which the pressure around the column is reduced to less than 0.1 mTorr.[78–80] With this device, less than 1% of total heat generated due to viscous friction is lost to the environment, which reduces the magnitude of the radial thermal gradient and can increase chromatographic efficiency by 35% under UHPLC operating conditions. However, even with a perfectly adiabatic system, heat flow through conductive parts of the overall column body can still lead to performance loss due to viscous friction, and further consideration on the materials used for column hardware and stationary phase supports is still needed to further eliminate such losses.[81]

Increased diagnostic feedback of various system parameters has been adopted in some modern UHPLC instruments, especially to simplify and automate troubleshooting. An example of this strategy is the "Analytical Intelligence" platform that combines a series of hardware and software controls that simplify instrument operation for less experienced users.[82] One feature is the use of a pressure diagnostic feature that detects air in the mobile phase based on system pressure fluctuations, which then stops the sample injection sequence to self-prime the system before continuing subsequent chromatographic runs.[83] Another diagnostic tool uses a built-in system balance to calculate mobile-phase consumption based on mass rather than a user-programmed volume, and once the mobile-phase reservoir is depleted the pump is halted.[84] Mobile-phase monitoring can also be achieved through the use of hydrostatic pressure measurements to determine the amount of liquid volume remaining in a reservoir.[85,86] Finally, system-user interfaces can be used to help control automated leak testing of various components in the fluidic path,[87] and provide specific maintenance instructions directly within this interface.

## 2.3 | Emerging detectors and hyphenation to mass spectrometry

Smaller column dimensions used in UHPLC require a reduction in overall system volume to limit extra-column broadening effects, so the absorbance flow cells that are used in modern UHPLC instruments are designed to maximize sensitivity while minimizing dispersion. The most common change from HPLC flow cells has been the adoption of light-pipe technology, in which the cell walls are coated with a reflecting material that increases the amount of light that is transmitted through the optical pathlength.[88,89] This permits the creation of smaller diameter, longer flow cells that maintain high detector sensitivity,[90] which can be further improved using data deconvolution techniques.[91] Multiple instrument vendors have also released flow cells with pathlengths on the order of 60-85 mm to increase the signal-to-noise ratio by a factor of 5- to 15-fold compared to standard 10 mm pathlength cells.[92–94] Recent investigations by Dasgupta *et al.*[95] and Vanderlinden *et al.*[96] have shown that the dispersion contribution by the detector cell is also slightly affected by the applied flow rate, and is a function of flow cell volume. An additional consideration is the need for higher data acquisition rates to obtain a sufficient number of data points across peaks from methods that generate much narrower bandwidths than observed in HPLC. Undersampling of peaks can lead to deformed peak shapes, potential loss in sensitivity, and added contributions to band broadening. The rule of thumb of obtaining at least 30 – 40 points across a chromatographic peak ensures that the true peak shape is obtained during detection.[97] This corresponds to acquisition rates in excess of 60-80 Hz are required for peak widths of 0.5 s, which can feasibly be observed in modern high-efficiency, high-throughput gradient separations. Most modern UHPLC absorbance detectors have acquisition ranges of 80-200 Hz to accommodate these conditions. Fast acquisition rates are most effective when coupled with small detector time constants that are related to embedded signal filters, as a high time constant (2.0 s) at 100 Hz acquisition rate can reduce the measured peak efficiency by 90%.[97] Advanced peak analysis algorithms have improved the capability of detecting unresolved peaks. Broad absorbance spectra obtained using diode array detection can be used to help deconvolute overlapping peaks that are not resolved through chromatographic separation, with the ability to digitally separate peaks with detected resolution factors down to 0.6.[98,99] New approaches to mathematically increasing the separation of partially resolved peaks have also been developed, including the use of power law transforms[100–102] and derivative enhancement data treatments[103] to digitally enhance

the separation between peaks with detected resolution factors as low as 0.5.

For molecules that do not contain a chromophore, so called universal detectors like charged aerosol detector (CAD), condensation nucleation light scattering detectors and evaporative light scattering detectors (ELSD) can be employed. A recent review by Zhang provides an overview of the drawbacks and benefits of all three detectors.[104] Apart from its higher detection sensitivity and reproducibility over ELSD, CAD methods are directly transferable to mass spectrometry. Schilling and Holzgrabe reviewed the application of CAD in pharmaceutical analysis.[105] The quantitative analysis of plant sterols and stanols using a tandem UV/CAD method at a system pressure of almost 800 bar was realized under 8 min.[106] Schilling has performed an extensive systematic variation of CAD settings for polysorbate analysis at UHPLC conditions.[107]

In addition to absorbance detectors and aerosol-based detectors, mass spectrometry is the other key detection mode most frequently interfaced to UHPLC instruments.[108] The lower flow rates that are commonly used with 2.1 mm i.d. UHPLC columns provide an improvement over older HPLC-MS interfaces, as the need for flow splitting that was common at flow rates in the 1 – 3 mL/min range is eliminated.[109] Contemporary electrospray ionization (ESI) sources are easily coupled to UHPLC column outlets, and as UHPLC-MS typically employs gradient methods that lead to some analyte trapping on the head of the column, the biggest issue in ensuring optimal chromatographic performance when coupling the two techniques is ensuring limited volume of connecting tubing between the column and ESI source.[110] As with absorbance detectors, high data acquisition rates in UHPLC should be maintained, although this can be a more significant challenge with MS due to longer duty cycle times for these instruments. Depending on the type of mass analyzer that is used, typical MS duty cycle times are on the order of 0.025 – 0.1 s, which limits data acquisition rates to a maximum around 40 Hz.[111] Newer time-of-flight (TOF) instruments have expanded this range up to 100 Hz, which can better facilitate narrow chromatographic peak widths provided by UHPLC technology.[112] For the increasingly popular Orbitrap instrument, there is a trade-off between duty cycle and resolving power,[113] with the total scan time also playing a role in overall method sensitivity.[114] For quantitative UHPLC-MS measurements, achieving 12 – 15 points per peak often provides sufficient information, with the added analyte selectivity over absorbance detection being deemed far more critical than slight peak undersampling. In high-throughput screening approaches using MS, this becomes less of an issue, as typically the separation column is either replaced with a small SPE cartridge or removed from the flow path completely.[115,116] The other challenge with coupling UHPLC to MS can be ion suppression effects due to sample matrix and/or LC mobile-phase components.[117]

## 3 | MULTI-DIMENSIONAL LC WORKFLOWS

Historically, offline 2D-LC – where fractions are collected at the outlet of one column and re-injected into a second column having orthogonal selectivity – have been used commonly for a wide variety of applications. Executing 2D-LC separations online, such that the first and second separations are carried out very close in time in a closed system, has the advantage that the risk for contamination during handling of fractions outside of the system is minimized.[118] In this section, we focus on recent advances in online 2D-LC separations. Readers interested in a more detailed comparison of offline and online 2D-LC separations are referred to.[119,120]

### 3.1 | Modulation strategies

As dilution related to the chromatographic process negatively affects separation performance and sensitivity in liquid chromatography, it is critically important to minimize its impact in order to enhance the separation power of LC×LC. The interface between the two separation dimensions is a key element that needs to be carefully optimized, as injection band-broadening due to improper selection of the modulation conditions can significantly reduce the overall peak capacity. In recent years, many groups and manufacturers have introduced different solutions that allow to modulate sample fractions between the first- and second-dimension analysis. The ultimate goal is to allow for a robust and miniaturized system (with respect to peak dispersion characteristics), that enables more sensitive multi-dimensional separations with improved solvent compatibility between the dimensions.

#### 3.1.1 | Multiple heartcutting 2D-LC (MHC or mLC-LC)

The initial application of 2D liquid-phase separation demonstrated using columns was heartcutting (LC-LC), where a single fraction of effluent from the 1D column is transferred to a $^{2}$D column for further separation.[121] In the early 2010s, proof-of-concept 2D-LC separations involving multiple heartcuts across a single 1D separation where shown by Zhang et al.[122] This approach has become known as multiple heartcutting (MHC, or mLC-LC), and has become quite popular among users of 2D-LC in recent years. While it is possible to carry out a MHC separation by using the same hardware as utilized in LC-LC, the latter has the significant limitation that the 2D separation of one heartcut must be completed before the next heartcut can be transferred to the 2D column. Here, we focus on an advanced version of MHC that allows temporary storage of fractions of 1D effluent in the interface used to connect the two dimensions of the system. This has the advantage that fractions from the 1D separation can be captured and stored while running 2D separations of previously collected fractions. This is described as "breaking the link between the timescales of the 1D and 2D separations," which enables operation of both dimensions of the system more efficiently.[123,124]

Figure 2 shows an example of an interface for MHC that enables collection of $^{1}$D effluent (blue paths) and $^{2}$D separation of fractions (red paths) in parallel. Two parking decks (A and B) bear several sample loops that are prepared to store fractions of $^{1}$D effluent. The decks are connected to the central 2D-LC modulator valve that controls which of

doi.org/10.1002/ansa.202100007


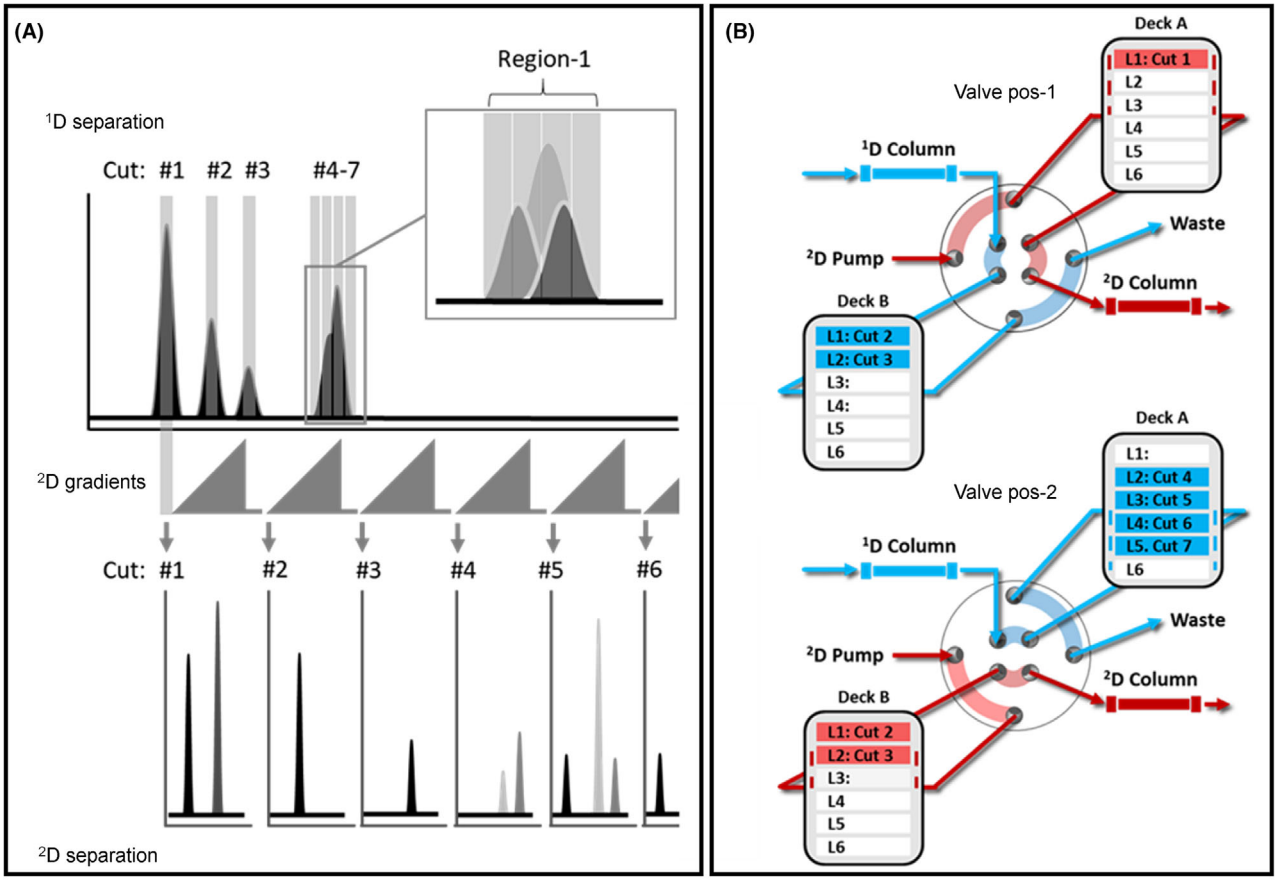


**FIGURE 2** Interface for MHC 2D-LC separations. Panel (A) depicts 1D and 2D chromatograms, and panel (B) the sampling/parking and analysis schedule. Heartcut #1 from the first peak in the 1D chromatogram was sampled in Loop-1 of Deck-A and is currently processed in the second dimension as shown by the 2D effluent flowing through this loop into the 2D column. Meanwhile, cuts #2 and 3 were parked in Loops 1 and 2 of Deck-B. The modulator switch from pos-1 to pos-2 placed Deck-B in the flow path for 2D separation, which simultaneously opened parking space in Deck-A

the decks are in the 1D and 2D flow paths at any given time. There are several possible ways to execute the separation illustrated in Figure 2 with respect to when and where the fractions of 1D effluent are parked, and when they are subsequently analysed in the second dimension. In the particular case shown here, the algorithm controlling the operation of the interface follows rules that prioritize minimizing the total number of valve switches, but also prompt processing of cuts with the goal of opening a deck for further parking as soon as possible. A different algorithm could iteratively recalculate the parking/$^2$D-analysis process with the goal to analyze as many cuts as possible.

### 3.1.2 | Selective comprehensive 2D-LC (sLC×LC, or HiRes)

The interface illustrated in Figure 2 can also be used for a mode of 2D-LC separation referred to as selective comprehensive (sLC×LC), or High Resolution Sampling (HiRes) 2D-LC.[123–125] Figure 2, panel (B) shows that Deck-A has sampled a region of interest (Region 1) in loops 2-5 (Cuts #4-7) and remains in flow through position (here loop 6) until $^2$D separation of fractions stored in Deck-B is complete. This approach has several potential benefits that are particularly useful for certain applications. First, this mode enables quantitative sampling of 1D peaks or regions embracing large volumes without having to change to very large loops in the sampling interface. For example, a $^1$D peak that is 10 s wide, with a flow rate of 1.0 mL/min. has a volume of about 165 µL, which could be sampled using a single 180 µL loop. Handling an injection of 180 µL into a 2D column can be challenging but could be enabled using special equipment (see section ASM). Alternatively, the sLC×LC/HiRes approach allows the same peak to be sampled using five 40 µL loops by making five adjacent cuts in the manner shown in Figure 2. A second major benefit is that comprehensively sampling a 1D peak allows for a better understanding of peak elution properties. In the 1D chromatogram shown in Figure 2, it can be observed that the medium grey peak elutes at the front of the three peaks co-eluting in Region 1. If a single heartcut is made in this region, there is no way to know where the three peaks observed in the subsequent $^2$D separation elute in relation to each other in the $^1$D separation. On the other hand, the four 2D chromatograms for cuts 4-7 clearly show that the medium grey peak elutes first in Region 1. This type of information can provide insights useful in the identification of unknown analytes. Finally, the ability to make multiple cuts across

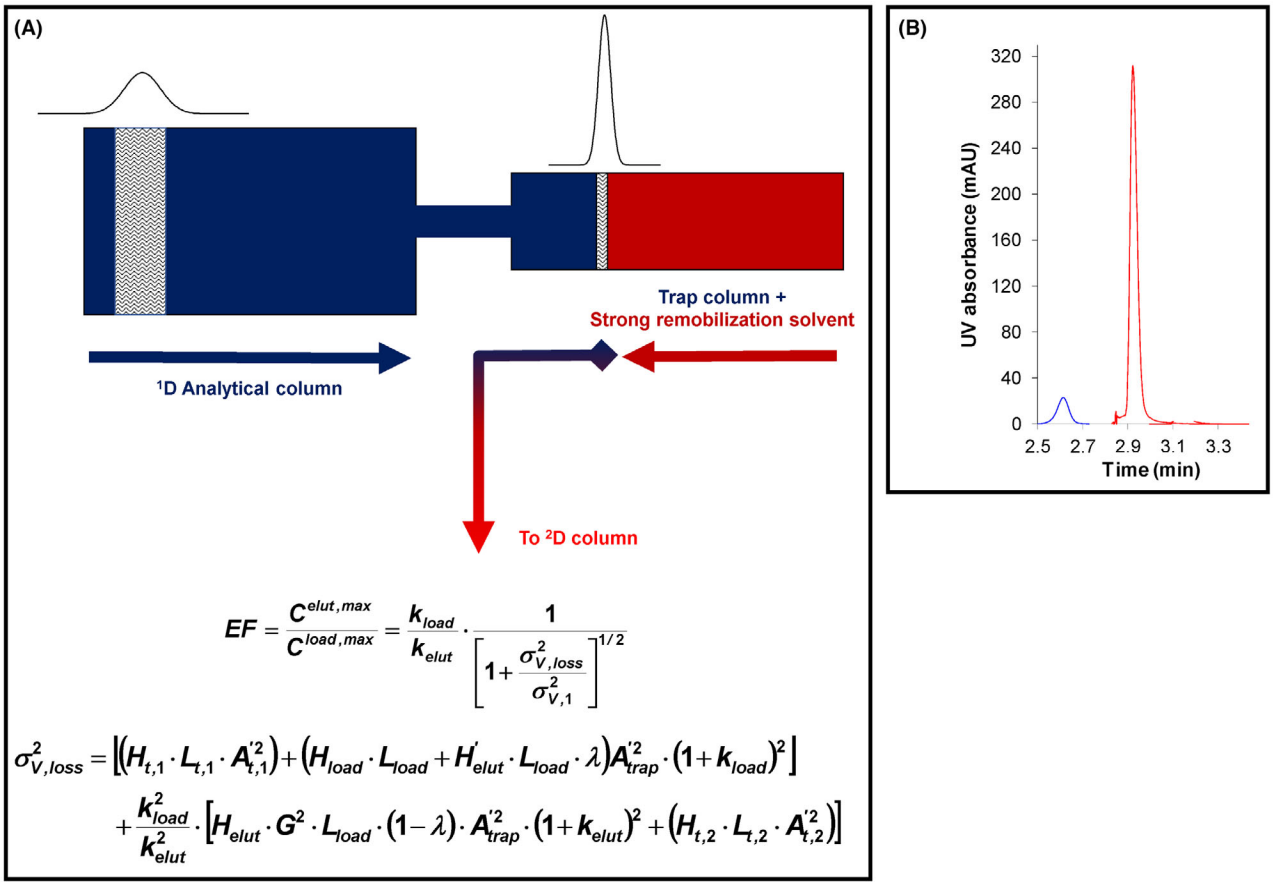


**FIGURE 3** Post-column refocusing using a trap column and strong-eluent remobilization. A, Overview of the changes in volumetric band variance σšV during the post-column refocusing process. B, Practical demonstration of the signal enhancement achieved resulting from post-column refocusing for the separation of an antibiotics sample. Furazolidone was brought to a 1 mm i.d. Hypercarb trap column (red signal) after eluting from an analytical 100 mm × 2 mm i.d. column packed with 3 µm fully-porous silica C18 particles (blue signal). Adapted from 129 with permission (© 2016, Elsevier B.V.)

a region of interest in the first dimension (*ie*, easily sampling a large window of 1D time) provides a defense against shifts in 1D retention time that can occur from one analysis to the next. This is especially important for molecules such as peptides and proteins whose retention is very sensitive to mobile phase composition and certain instrument parameters.[126]

### 3.1.3 | Post-column refocusing

The implementation of trapping columns, packed with retentive particles, as the modulator offers the possibility to amend the solvent compatibility between both dimensions and reduce chromatographic dilution. In this process, the compounds eluting from the 1D analytical column are directed to a trapping column (see Figure 3A). Next, a strong solvent is used to direct the trapped peak towards the 2D column, inducing a peak focusing effect. An in-depth theoretical study of peak refocusing, using a trap column and subsequent strong-eluent elution, was performed by De Vos *et al.*[127] Mathematical expressions that describe the optimized properties of such a modulator are described, resulting in an expression that shows which parameters are most critical to the peak focusing effect (see Figure 3A). This concomitantly results in a signal enhancement of the trapped analyte, drastically improving the limit of detection. It is important to use trap columns packed with small particles, resulting in small plate heights, and minimize the i.d. and length of the connection tubing. The achievable concentration enhancement can also be increased by reducing the diameter and the length of the trap column. The employed solvents should induce strong retention during the trapping process, while the remobilization should be performed using mobile phase systems with a high solvent-strength (*i.e.*, acetonitrile or methanol in RPLC mode). The latter recommendation can result in detrimental viscous fingering effects, which should be addressed. The generic post-column refocusing approach, and its different parameters, were studied under isocratic and gradient reversed-phase conditions amounting for signal enhancement factors of well over one order of magnitude.[128,129] Figure 3B shows the result of post-column refocusing performed on an antibiotics sample in gradient elution mode, enhancing the detection sensitivity with a factor of 14.

Altering the temperature during trapping and eluting can enhance the peak focusing effect of non-thermolabile analytes. A cryogenic thermal modulator interface at the column outlet was described by

Eghbali *et al*., to demonstrate peak focusing of protein and peptide samples.[130] The device provided a cold gas flow (-20°C) around the column housing to trap components, followed by the introduction of boiling water as a heating agent to initiate a strong peak focusing effect resulting in an increased S/N ratio. Another way of implementing thermal modulation interfaces was demonstrated by Verstraeten *et al*., who studied the use of a low thermal mass heating sleeve as a preconcentration device and injector for the second dimension column of an LC×LC set-up.[131] This concept was revisited by the Weber group, who demonstrated the use of a multiplicative thermal focusing device for on-column focusing.[132]

### 3.1.4 | Active solvent modulation (ASM) to address mobile phase mismatch

In 2D-LC, the modulator collects a portion of 1D effluent, which then becomes the sample for a subsequent 2D separation. If there is a significant mismatch between the 2D mobile phase and the sample received from the first dimension, severe effects can occur including dramatic distortion of 2D peaks, analyte breakthrough, and losses in resolution and sensitivity.[133–135] This sometimes leads to the description of particular combinations of separation types as being "incompatible" for 2D-LC.[136] What constitutes "significant mismatch" often depends on the application, but can be related to differences in mobile phase properties including solvent strength, polarity, viscosity, or pH. For instance, components of a sample injected onto a reversed phase column may be insufficiently retained if the sample matrix (*eg*, 1D effluent) contains a high fraction of organic solvent.[137] The effect becomes more pronounced with increasing injection volume, decreasing volume of the 2D column, or a decrease in the general retentivity of the 2D column. These challenges have been recognized for a long time, and research groups have explored different potential solutions. These include schemes based on evaporation to control the level of organic solvent in samples delivered to the second dimension,[138–140] approaches based on adsorption to separate analytes from the sample matrix prior to the 2D separation,[131,141] and active dilution of the $^{1}$D effluent with weak solvent.[134] All of these approaches share the common aim to increase retention of analytes of interest at the 2D column inlet. Recent work focused on the development of an approach referred to as Active Solvent Modulation (ASM).[134] This is a valve-based approach that allows for dilution of 1D effluent fractions contained in loops of the 2D-LC interface with weak solvent prior to transfer to the $^{2}$D column for further separation. In ASM the weak solvent is provided by the same $^{2}$D pump that is used to drive the eventual $^{2}$D separation. This can result in significantly improved chromatography in the second dimension, especially in cases where analytes of interest can be focused at the $^{2}$D column inlet. ASM has successfully been employed in a variety of applications ranging from low to high molecular weight compounds including peptides, proteins, organic polymers, and monoclonal antibodies (mAbs).[142–144]

Figure 4A shows an example of the effectiveness of ASM for mitigating mobile phase mismatch effects in the context of a 2D-LC separation of subunits of mAbs.[143] In this case, the 1D separation relies on the HILIC mode of separation, which is highly selective for different mAb subunit glycoforms. The 2D separation relies on the reversed-phase mode of separation, which is effective for rapid separation of the three mAb subunits (Fc/2, LC, and Fd) that result from digestion with the *IdeS* enzyme, followed by digestion with dithiothreitol (DTT). Separation of these molecules requires about 70% ACN in the HILIC mobile phase, and about 30% ACN in the reversed-phase mobile phase. As one might expect, this mismatch in %ACN levels leads to severe breakthrough in the second dimension unless something is done to prevent it. Figure 4A shows the 1D HILIC separation of the subunits of the mAb atezolizumab following digestion with IdeS and reduction with DTT. Figure 4B shows the corresponding 2D chromatogram obtained when fractions of 1D effluent are directly injected into the 2D column. Severe breakthrough of protein peaks is apparent around the dead time of the 2D column, as highlighted by the red rectangle. On the other hand,

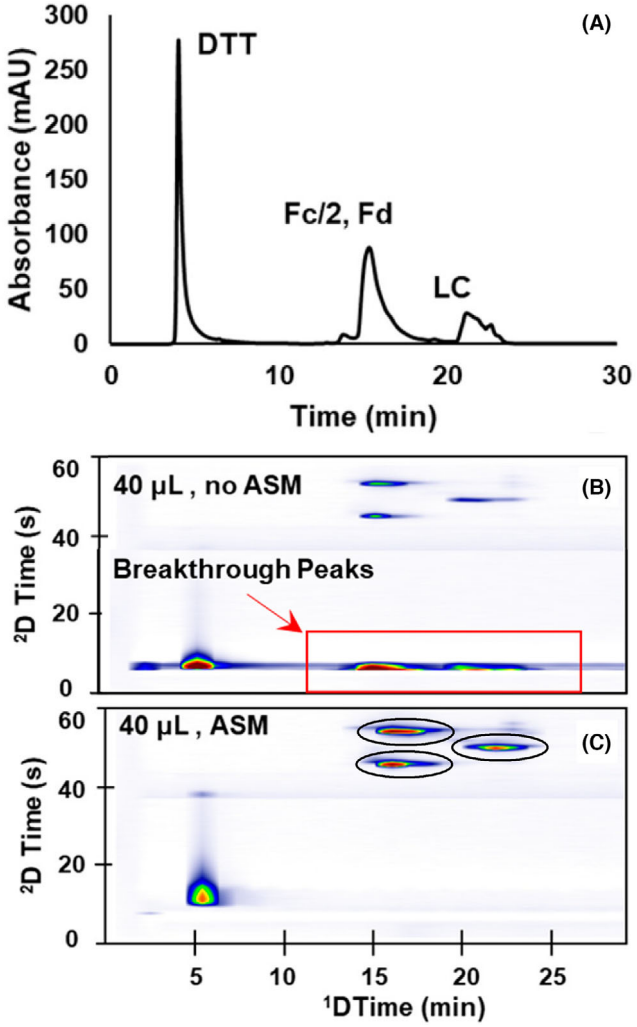


**FIGURE 4** 2D-LC separations of the fragments of the monoclonal antibody atezolizumab after reduction with the IdeS enzyme and reduction with dithiothreitol. A, 1D chromatogram obtained from a HILIC separation of these fragments; B, 2D chromatogram obtained without ASM; C, 2D chromatogram obtained with ASM. Adapted from 143 with permission (© 2018, American Chemical Society)

when ASM is activated with an ASM factor of 3 (*i.e.*, nominally a three times dilution of the 1D sample prior to it hitting the 2D column), the breakthrough peaks are completely eliminated and the protein peaks are retained and nicely resolved as shown in Figure 4C.

### 3.2 | Novel modulator technology

As discussed in a previous section, critical parameters in stationary-phase assisted focusing include the i.d. of trapping segment, and the extra-column dispersion once peak compression of remobilized analytes have been achieved by a strong solvent front. To maximally benefit from the peak focusing effect, De Vos *et al.* reported on the development of a microfluidic modulator chip, compatible with commercially available valve switching technology at UHPLC conditions, to transfer sub-microliter fractions in an on-line 2D-LC workflow.[145] Peak shapes and dispersion characteristics were assessed with and without the presence of a monolithic mixing entity, that can also be employed to enable stationary-phase focusing of analytes between the 1D and 2D developments. Additionally, the application of the modulator chip was demonstrated in a heart-cut SCX-RPLC-nanoESI-MS workflow for the targeted analysis of a signature peptide in a protein digest. Wei and co-workers recently developed a sample treatment platform that incorporates a microfluidic chip platform for protein reduction and alkylation, offering a versatile reactor prior to MS detection.[146] Yin *et al.* developed a polyimide chip device with integrated ESI spray, fitting between the stator and the rotor of a switching valve, to realize switching between a reversed-phase separation column and an enrichment column for the identification of peptides from a BSA digest.[147] This chip concept was recently adopted and expanded by the Belder group, where a full-body fused silica chip device with monolithic ESI emitter was used for on-chip 2D-LC/MS of a pesticide mixture and a tryptic digest.[148] The Schmitz group recently reported modulator, called "at-column dilution modulator", by adding an additional transfer pump to the interface. The latter can modulate 1D sample fractions, which are afterward mixed with the 2D gradient flow before reaching the 2D column. This device allows to modulate the dilution factor by adjusting the transfer flow rate and composition independent of the operating conditions used during the 1D and 2D analysis.[149–151]

### 3.3 | Spatial 2D- and 3D-LC separations

Spatial comprehensive multi-dimensional liquid chromatography entails a chromatography concept that has the capability to yield high resolving power within a short analysis time, in which the analytes are migrating to different positions in a 2D plane or in a 3D space. High resolving power can be achieved given that the maximum peak capacity is the product of the three individual peak capacities. Short analysis times, and hence high peak-production rates, are realized as the second-dimension and third-dimension separation stages are performed in parallel, overcoming the fundamental limitation of conventional multi-dimensional approaches, in which sampled fractions are analyzed sequentially. A well-known example of a spatial 2D-LC analysis is iso-electric focusing followed by a separation based on mass-to-charge ratio utilizing SDS-PAGE. After the first-dimension development in an IEF strip (x-direction) all analyte fractions are separated in parallel in the z-direction.

An early protype chip for spatial comprehensive 3D-LC was introduced in 2015, featuring interconnected parallel channel structures for the 2D and 3D development containing monolithic stationary phases and a radially-interconnected 2D and fractal 3D flow distributors allowing for homogeneous flows across all channels, see Figure 5A–C.[152,153] Different approaches have been pursued to design the microfluidic chip device, allowing to distribute flow and to confine flow in spatial multi-dimensional LC during subsequent developments. A new concept to confine flow during the $^{1}$D stage within a cylindrical tube containing through-holes was introduced in 2018.[154,155] In this device, the development of a $^{2}$D stage was enabled after aligning the through holes of the cylindrical $^{1}$D tube with the 2D flow distributor and $^{2}$D channels. Adamopoulou *et al.* developed a device using 3D-printing technology which was tested at flow rates in the range of 0.5 to 5 mL/min.[156] Themelis *et al.* reported on a microfluidic device with on-chip active valving, enabling the leak free operation at high pressures.[157] By integrating monolithic stationary phases in the microchannels for the $^{2}$D development, stationary-phase focusing of analytes was demonstrated at the channel inlets, improving sensitivity, see Figure 5D-F for the chip design and subsequent active-valving including analytes focusing steps. The same group demonstrated the use of physical barriers, *i.e.* constrictions inside the microchannels of the chip and integration of monolithic stationary phases, to block chip segments during the $^{1}$D development.[152] Adamopoulou *et al.* investigated the use of permeability differences across different compartments to restrict flow using computational fluid dynamics (CFD) simulations.[158] Additionally, a novel 3D flow distributor design was proposed connecting one 2D flow distributor to parallel 2D flow distributors allowing to feed the 3D stage.[159] The use of parallel electrochemical detection with carbon fibers as working electrodes placed at the outlets of a separation device with four parallel channels was explored by Komendova *et al.*[160] The latter approach may be a possible route to establishing detection in an array of $^{3}$D channels in a spatial 3D-LC chip. While spatial 3D-LC is still in its infancy, general considerations for chip design and possibilities and prospects to establish spatial comprehensive 3D-LC analysis have recently be discussed by Themelis *et al.*[161]

## 4 | RECENT KEY APPLICATIONS

### 4.1 | Increasing sample throughput and resolution in 1D-LC

Kresge *et al.* reported on a high-throughput UHPLC approach allowing to complete a 24-run sequence to identify linearity, recovery, and repeatability for both drug assay and impurity analysis in 16 min, corresponding to 40 s consecutive injections.[71] Experiments were

Review
doi.org/10.1002/ansa.202100007
Chemistry Europe
European Chemical Societies Publishing

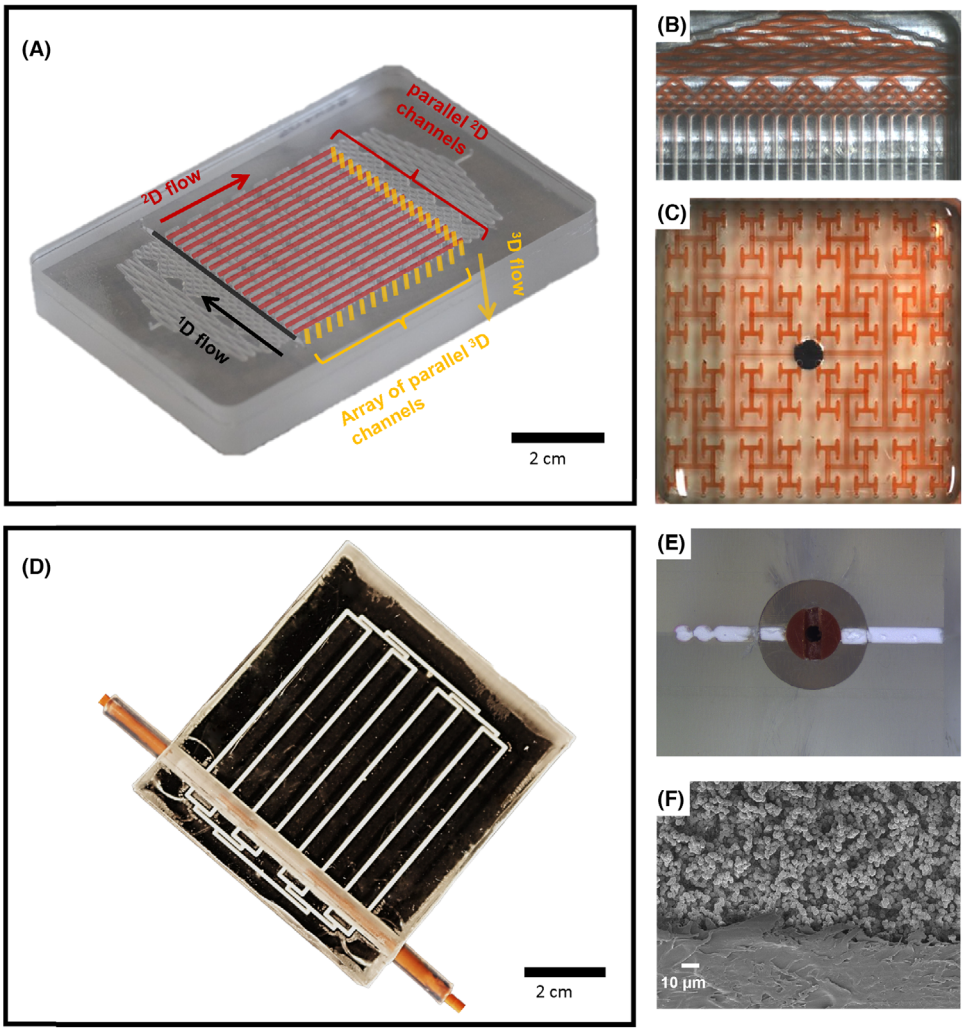


**FIGURE 5** Technological advances for the realization of spatial 3D-LC. A, First prototype chip for spatial 3D LC integrating an interconnected channel design and 2D and 3D flow distributors, zoom-in panels in (B) and (C) show the channel layout for the 2D and 3D stages, respectively. Reproduced from 152 and 153 with permission (© 2015, The Royal Society of Chemistry and © 2015, John Wiley and Sons). Panel (D) shows a spatial 2D-LC integrating active valving, to confine the flow during the 1D stage, and polymer-monolithic stationary phases allowing to focus analytes at the 2D channel inlets prior developing the 2D gradient. The zoom-ins show (E) a cross section of a spatial chip that integrates the active-valving concept with a polymer monolith present in the 2D flow distributor and parallel 2D channels, and (F) shows the attachment of the polymer monolithic material to the chip substrate. Reproduced from 157 with permission (© 2020, Elsevier B.V.)

performed using a 2.1 × 100 mm long column packed with 2.7 µm $C_{18}$ particles, providing higher resolution compared to a 50 mm long column, while operating at high linear velocities to promote throughput. Higher sequence speed was ensured by preparing injections during preceding runs. Compared to the pharmacopeial monograph describing a conventional HPLC analysis, a 25-fold increase in throughput was achieved. In hydrophilic interaction chromatography (HILIC) column equilibration is perceived as a disadvantage preventing high-throughput analysis. McCalley systematically investigated the effect of partial equilibration on chromatographic retention.[162] For a wide range of HILIC materials partial equilibration by purging with 12 column volumes of the initial mobile-phase composition resulted in precision in retention times in the range of 0.03 – 0.3%. It should be noted that it is critical to keep the equilibration period strictly constant. Berthelette *et al*. evaluated Multiple Injections in a Single Experimental Run (MISER) to study the column equilibration of HILIC columns.[163] In MISER, consecutive injection are performed while the separation is occurring, and hence without waiting for the initial separation to be completed.[164] Using 10% water instead of 5% water in the mobile phase a 5-fold reduction in equilibration volume was obtained. It was noted however that different equilibration profiles of the acidic, basic, and neutral probes differ. This suggested that HILIC column equilibration involved both the gradual build-up of the adsorbed aqueous layer and the buffer counter-ion layer on the particle surface. Hence, the mechanism of retention for these probes is dependent on the equilibration of the partitioning mechanism.[163] Schneider *et al*. reported on the use of a multisampler with a dual-needle injection to reduce the overall analysis time for food preservatives by 60%.[65] The set-up was configured in such way that one column was employed for gradient run, while a second columns was regenerated in parallel. The same

principle was utilized by Carillo *et al.* who described high-throughput peptide mapping of a trastuzumab digest using a tandem LC-MS workflow.[165] Grosse *et al.* described a configuration in which two independent flow paths were realized using a sampler with dual-needle possibilities and two UV detectors for the quantitative analysis of water- and fat-soluble vitamins in drinks and food supplement tablets.[68] A similar approach was pursued for the analysis of acetaminophen impurities using the complementary RPLC columns extending the selectivity range.[69]

By increasing the operating pressure of UHPLC separations in excess of what is currently commercially available, high throughput separations with improved separation efficiency can be achieved. Sorensen *et al.* developed 15–50 cm long capillary columns packed with 1.7 µm $C_{18}$ particles and applied these in gradient mode for the analysis of lipid isomers and complex lipid extracts from human plasma.[166] To overcome longitudinal diffusion the 50 cm long columns were operated at pressures as high as 2400 bar, allowing to reach peak capacities up to 410 within a 4 h gradient.

## 4.2 | Multidimensional LC workflows

In recent years, the use of 2D-LC has evolved from being a focus of primarily academic researchers, to being adopted by a wider community including users in the chemical industry and the life sciences. The drivers for this evolution include the continually increasing complexity of samples encountered in these markets, and the availability of commercially available 2D-LC systems with integrated software solutions. Successful implementation of 2D-LC methods over time requires the development of method development strategies that can be carried out by a wide variety of users; this has historically been a significant barrier to wider use of 2D-LC.

Conventional 1D-LC can be used to identify differences in selectivity for a set of analytes of interest by screening a set of pre-determined chromatographic conditions (*eg*, stationary phase type, mobile phase type, pH, temperature) in a highly automated way. Using this 1D-LC screening step, candidate selectivities can be implemented in a 2D-LC separation leading to an improved complementary method that

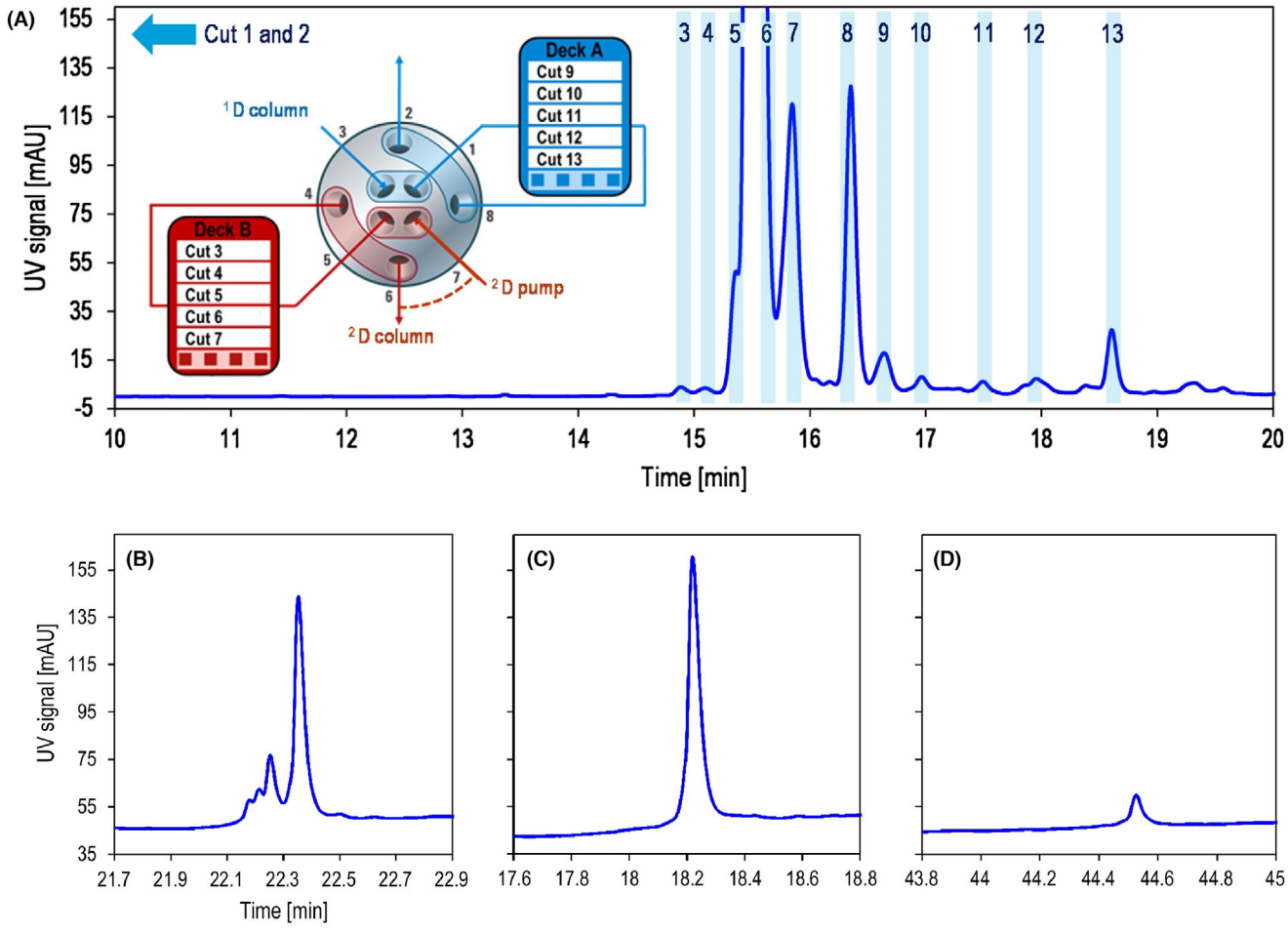


**FIGURE 6** Example of MHC 2D-LC used to characterizate of related peptide impurities. Panel (A) shows a 1D separation of peptides by reversed-phase with a buffer containing ammonium phosphate and sodium sulphate. 2D separations of fractions from cuts (B) #7, (C) #8, and (D) #13, respectively. The 2D separations both desalt the fractions prior to MS detection, and provide additional separation in cases where multiple peptides co-eluted in the first dimension. Reproduced from 126 with permission (© 2020, Elsevier B.V.)

doi.org/10.1002/ansa.202100007


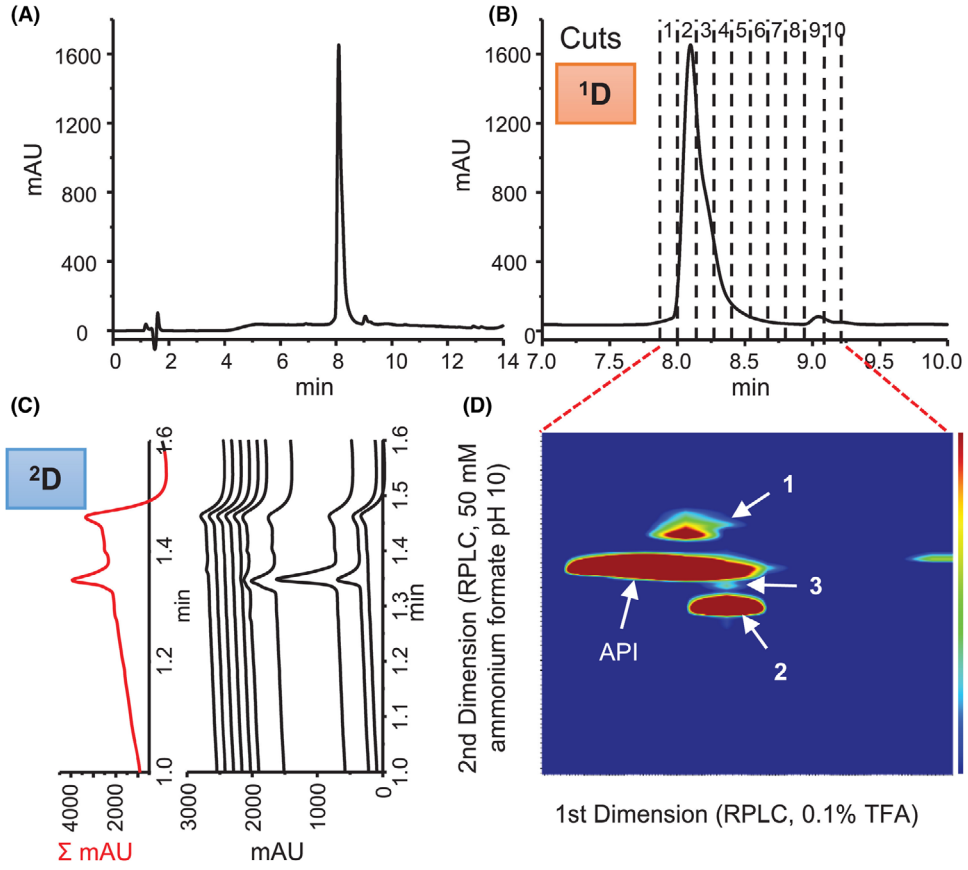


**FIGURE 7** Example of sLC×LC applied to characterization of impurities in a synthetic peptide active pharmaceutical ingredient (API). A, Full-scale 1D chromatogram obtained using a reversed-phase separation at low pH for the API material. B, Zoom-in showing region of 1D separation sampled by sLC×LC using ten cuts to cover the region of interest. C, 2D chromatograms (reversed-phase at high pH) obtained by UV detection. D, Same data as in Figure 7C, but in the format of a 2D contour plot. Reprinted from 142 with permission (© 2020, Elsevier B.V.)

can achieve sufficient resolution for the separation of specific target analytes.[167] This approach works best for samples of low complexity, especially when analytical standards for all of the analytes of interest are available, but it can also be useful for complex samples when the analysis is focused on a limited number of target compounds. Finding the appropriate combination of stationary phases for the application at hand is time-consuming, and also method robustness is affected when sub-optimal separation conditions are selected.[168]

### 4.2.1 | Recent applications of MHC and HiRes 2D-LC

Figure 6 shows an example of an application that benefits from the collection of 1D effluent fractions and 2D separation in parallel.[126] Figure 6A shows that the peaks labeled 3-7 are too close together in time to allow high-resolution 2D separations in between the times when the cuts for these peaks are made. However, when the link between the timescales of 1D sampling and $^2$D separation is broken, a total of 13 heartcuts can be made, and subsequently separated in the second dimension, all in a single 2D-LC analysis. In this particular case, peptides resulting from degradation of bovine insulin are first separated by reversed-phase using an ammonium phosphate buffer including sodium sulphate salt. Then, in the second dimension, the components of each fraction are separated by reversed-phase, but with a MS-compatible formic acid containing mobile phase. The second dimension both, allows separation and diversion of salts to waste around the dead time of each $^2$D separation, and further separation of peptides that had co-eluted from the 1D separation (*eg*, see Figure 6B).

Figure 7 shows an example of a recent application that benefited from the sLC×LC mode of 2D-LC to produce a high resolution 2D chromatographic view of impurities present in an active pharmaceutical ingredient (API) that is a synthetic peptide.[142] Panel A shows the chromatogram that was obtained by reversed-phase LC with a low pH (0.1% TFA) mobile phase. As expected, the chromatogram is dominated by a single large peak, since this material had been previously purified under similar chromatographic conditions. However, upon looking more closely at this peak – as in Panel B – a shoulder is evident on the rear of this main peak. The sLC×LC approach was used to collect ten fractions covering this entire region of interest. Panel C shows the individual $^2$D chromatograms from these fractions, and Panel D shows the contour plot constructed from the same ten chromatograms. The contour plot quickly and obviously shows two major impurities eluting in the tail of the main peak. Readers interested in learning more about

how other groups have used these approaches are referred to an online database of 2D-LC applications.[169]

### 4.2.2 | Advanced multi-dimensional characterization systems

Recently, Regalado and co-workers discussed the addition of multiple selector valves to a conventional 2D-LC-MS system. This approach enables screening of multiple column and mobile phase chemistries in both separation dimensions in a completely automated fashion, allowing for rapid screening of different column/eluent combination without user intervention.[170] Simplified method development was successfully demonstrated for multicomponent mixtures of drug substances, the separation of which was challenging because ingredients were closely related (as is often the case with API-related impurities).[126,171] The methods employed were run under standard gradient conditions for initial screening purposes and once good column mobile phase combination were defined, it was suggested that further optimization of multiple chromatographic parameters should be performed using computer-assisted modeling. An example of the latter has been published very recently by the same group.[172]

Recently, researchers used multi-dimensional separation methods to characterize protein biopharmaceuticals. These large molecules (*e.g.* a monoclonal antibody (mAb) has a mass of ca. 150 kDa) can be highly heterogeneous with a myriad of possible variants that may coexist and impact safety and efficacy of the drug. Such structural complexity poses enormous demands on instrumental analysis. A recent report by Stoll and co-workers demonstrates the advantage of HILIC × RPLC-MS over IEX × RPLC for the determination of glycosylation in three different mAbs. Active solvent modulation was implemented to improve detection sensitivity and eliminate 2D injection breakthrough.[143] By the incorporation of data arising from ion-mobility-MS (IMS) detection, it is possible to extend the information obtained from 2D-LC separations into so-called four-dimensional methodology.[173–176] The fast cycling time of commercially IMS equipment made it suitable for sampling the 2D-analysis without compromising separation performance.[177] Some groups have added additional dimensions to automate the characterization of proteins.[178,179] An online reduction and digestion step was integrated, using an RPLC column and an immobilized trypsin

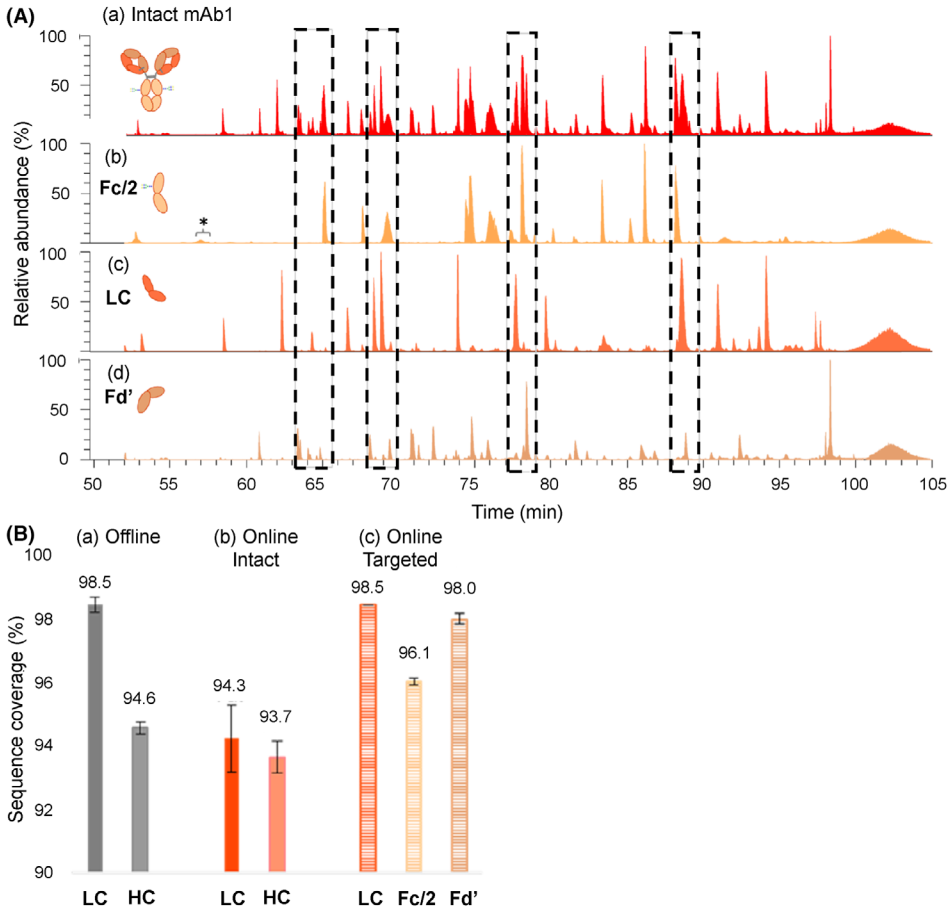


**FIGURE 8** Application of an automated targeted bottom-up strategy. A, Total ion current chromatograms obtained for RPLC-MS peptide mapping of the intact mAb1 and its respective fragments ((a) Fc/2, (b) LC, and (c) Fd'). The rectangles highlight the better resolving power for the targeted analysis. B, Performance of digestion for the (a) classic offline digestion compared with the novel online workflow performed on (b) the intact mAb and (c) the targeted bottom-up approach on the fragments. Reproduced from 181 with permission (© 2020, American Chemical Society)

cartridge respectively, combined with a multi-column workflow to monitor post-translational modifications in therapeutic mAbs.[179] The same group has built a similar set-up that couples an immobilized IdeS-enzyme column, which realizes a limited digestion of mAbs into Fab and Fc in only 10 min, to a HILIC-MS workflow. This new online workflow was compared with a conventional offline procedure, allowing to study glycosylation patterns of mAbs with run times of about 1.5h.[180] In a recent contribution the authors have extended this workflow with a trypsin digestion cartridge to allow for targeted RPLC-MS peptide mapping.[181] PTMs of the mAb are monitored using a bottom-up approach, while also characterizing individual mAb fragments, as shown in Figure 8A. The targeted analysis approach resulted in better resolved peptide peaks (marked by the rectangles) as a result of the higher efficiency of ionization. The good performance of the online digestion workflow is further demonstrated by displaying sequence coverage, showcasing a high sequence coverage of 96 – 99% for the fragments with a relative standard deviation lower than 0.25% (see Figure 8B).

## 5 | CONCLUDING REMARKS AND FUTURE PROSPECTS

UHPLC and multidimensional LC instrumentation have seen an impressive technological evolution during the past decade. Column manufacturers have also introduced columns packed with sub-2 µm particles – beyond the standard RPLC stationary phases – that assure a reliable toolbox for the chromatographer to tackle several analytical challenges using a variety of LC modes. Currently 2.1 mm i.d. columns are considered the state of the art. However, significant benefits can be realized by downscaling column dimension further, that is, minimize chromatographic dilution, reduction of solvent consumption (green chemistry), and enhanced flow rate compatibility toward (MS) detectors. However, this requires a step-change in instrument design, as extra column contributions need to be significantly reduced with over one order of magnitude. This also requires advances in injector technology and improvements in detection technology, without compromising S/N-ratios or acquisition times. Further decreasing column i.d. allows also to operate at slightly higher pressure, due to the reduced viscous heating contributions to band broadening, making it possible to operate at backpressures above 1500 bar.

Advancing modulator technology is required to further boost multidimensional LC workflows. The contrast with commercially available multidimensional gas chromatography equipment is still large. The utilization of post-column refocusing prior to the 2D development is not fully implemented yet, which will significantly advance resolving power and detection sensitivity. Furthermore, there are ample possibilities to further enhance the trap and release of molecules by implementing thermal modulation approaches. The software management system to control instrumentation for 2D-LC needs to be paired properly with method development software to optimize multidimensional separations.[182] Ideally, a graphical user interface that is intuitively simple for the less-experienced chromatographer, but at the same time allows to progressively tweak the separation conditions is most desirable. The advent of microfluidic technology and additive manufacturing will enable the development of novel solutions for spatial multi-dimensional 2D and 3D-LC workflows,[152] ultimately converging to a new leap in separation performance.

## ACKNOWLEDGMENTS

JPG acknowledges support for work in this area from the Chemical Measurement and Imaging Program in the National Science Foundation Division of Chemistry under Grant CHE-2045023. SE acknowledges research project G033018N and support of this work by an Excellence of Science grant (30897864) of the Research Foundation Flanders and the Fonds de la Recherche Scientifique (FWO-FRNS) is gratefully acknowledged. JDV acknowledges the FWO for support by a senior postdoctoral fellowship 12J6520N.

## ORCID

*Jelle De Vos* https://orcid.org/0000-0001-7880-9916

## REFERENCES

1. Giddings JC. *Dynamics of Chromatography. Part 1. Principles and Theory*. New York, NY: Marcel Dekker, Inc., 1965.
2. Giddings JC. Comparison of theoretical limit of separating speed in gas and liquid chromatography. *Anal Chem*. 1965;37:60-63. https://doi.org/10.1021/ac60220a012
3. Poppe H. Some reflections on speed and efficiency of modern chromatographic methods. *J Chromatogr A*. 1997;778(1-2):3-21. https://doi.org/10.1016/S0021-9673(97)00376-2
4. Desmet G, Clicq D, Gzil P. Geometry-independent plate height representation methods for the direct comparison of the kinetic performance of LC supports with a different size or morphology. *Anal Chem*. 2005;77(13):4058-4070. https://doi.org/10.1021/ac050160z
5. Broeckhoven K, Cabooter D, Eeltink S, Desmet G. Kinetic plot based comparison of the efficiency and peak capacity of high-performance liquid chromatography columns: Theoretical background and selected examples. *J Chromatogr A*. 2012;1228:20-30. https://doi.org/10.1016/j.chroma.2011.08.003
6. De Vos J, De Pra M, Desmet G, et al. High-speed isocratic and gradient liquid-chromatography separations at 1500bar. *J Chromatogr A*. 2015;1409:138-145. https://doi.org/10.1016/j.chroma.2015.07.043
7. Broeckhoven K, Desmet G. Advances and challenges in extremely high-pressure liquid chromatography in current and future analytical scale column formats. *Anal Chem*. 2020;92(1):554-560. https://doi.org/10.1021/acs.analchem.9b04278
8. Giddings JC. Two-dimensional separations: concept and promise. *Anal Chem*. 1984;56(12):1258A-1270A.
9. De Vos J, Broeckhoven K, Eeltink S. Advances in ultrahigh-pressure liquid chromatography technology and system design. *Anal Chem*. 2016;88(1):262-278. https://doi.org/10.1021/acs.analchem.5b04381
10. Eeltink S, De Vos J. Ultra-high-pressure liquid chromatography. In: Worsfold P, Townshend A, Poole C, Miró M, eds. *Encyclopedia of Analytical Science*. Amsterdam, the Netherlands: Elsevier; 2019:261-269.
11. Walter TH, Andrews RW. Recent innovations in UHPLC columns and instrumentation. *TrAC - Trends Anal Chem*. 2014;63:14-20. https://doi.org/10.1016/j.trac.2014.07.016
12. Fekete S, Schappler J, Veuthey J-L, Guillarme D. Current and future trends in UHPLC. *Trends Anal Chem*. 2014;63(September 2016):2-13. https://doi.org/10.1016/j.trac.2014.08.007

13. Bidlingmeyer BA, Hooker RP, Lochmuller CH, Rogers LB. Improved chromatographic resolution from pressure-induced changes in liquid-solid distribution ratios. *Sep Sci*. 1969;4(6):439-446. https://doi.org/10.1080/01496396908052271
14. Bidlingmeyer BA, Rogers LB. Investigation of pressure-induced changes in the chromatographic selectivity of methyl and ethyl orange on silica gel. *Sep Sci*. 1972;7(2):131-158. https://doi.org/10.1080/00372367208058978
15. Bidlingmeyer BA, Rogers LB, Bidlingmeyer BA. Steric-exclusion chromatography at pressures up to 3500 kilograms per square centimeter. *Anal Chem*. 1971;43(13):1882-1883. https://doi.org/10.1021/ac60307a047
16. Maldacker TA, Rogers LB. Steric exclusion behavior of sodium dodecyl sulfate at pressures up to 50000 psi. *Sep Sci*. 1973;8(6):627-645. https://doi.org/10.1080/00372367308056060
17. Maldacker TA, Rogers LB. Anion exchange behavior of bromide, chloride nitrite, and the lead(II)-nitrate system at pressures up to 3600 kg/cm2. *Sep Sci*. 1974;9(1):27-33. https://doi.org/10.1080/01496397408080041
18. Prukop G, Rogers LB. Reverse phase ion-pairing chromatography at pressures up to 345 MPa. *Sep Sci Technol*. 1978;13(1):59-78. https://doi.org/10.1080/01496397808057088
19. Prukop G, Rogers LB. Cation exchange at pressures up to 400 MPa. *Sep Sci Technol*. 1978;13(2):117-125. https://doi.org/10.1080/01496397808057094
20. MacNair JE, Lewis KC, Jorgenson JW. Ultrahigh-pressure reversed-phase liquid chromatography in packed capillary columns. *Anal Chem*. 1997;69(6):983-989. https://doi.org/10.1021/ac961094r
21. MacNair JE, Patel KD, Jorgenson JW. Ultrahigh-pressure reversed-phase capillary liquid chromatography: Isocratic and gradient elution using columns packed with 1.0-μm Particles. *Anal Chem*. 1999;71(3):700-708. https://doi.org/10.1021/ac9807013
22. Jerkovich AD, Mellors JS, Jorgenson JW. The use of micrometer-sized particles in ultrahigh pressure liquid chromatography. *LC-GC North Am*. 2003;21(7):600-610.
23. Patel KD, Jerkovich AD, Link JC, Jorgenson JW. In-depth characterization of slurry packed capillary columns with 1.0-μm nonporous particles using reversed-phase isocratic ultrahigh-pressure liquid chromatography. *Anal Chem*. 2004;76(19):5777-5786. https://doi.org/10.1021/ac049756x
24. Mazzeo JR, Neue UD, Kele M, Plumb RS. Advancing LC performance with smaller particles and higher pressure. *Anal Chem*. 2005;77(23):460A-467A. https://doi.org/10.1021/ac053516f
25. McCalley D V. The impact of pressure and frictional heating on retention, selectivity and efficiency in ultra-high-pressure liquid chromatography. *TrAC - Trends Anal Chem*. 2014;63:31-43. https://doi.org/10.1016/j.trac.2014.06.024
26. Broeckhoven K, Desmet G. Considerations for the use of ultra-high pressures in liquid chromatography for 2.1 mm inner diameter columns. *J Chromatogr A*. 2017;1523:183-192. https://doi.org/10.1016/j.chroma.2017.07.040
27. Carr PW, Wang X, Stoll DR. Effect of pressure, particle size, and time on optimizing performance in liquid chromatography. *Anal Chem*. 2009;81(13):5342-5353. https://doi.org/10.1021/ac9001244
28. Guiochon G, Gritti F. Shell particles, trials, tribulations and triumphs. *J Chromatogr A*. 2011;1218(15):1915-1938. https://doi.org/10.1016/j.chroma.2011.01.080
29. Gritti F, Guiochon G. Facts and legends on columns packed with sub-3-μm core-shell particles. *LCGC North Am*. 2012;30:586-595.
30. Liekens A, Denayer J, Desmet G. Experimental investigation of the difference in B-term dominated band broadening between fully porous and porous-shell particles for liquid chromatography using the Effective Medium Theory. *J Chromatogr A*. 2011;1218(28):4406-4416. https://doi.org/10.1016/j.chroma.2011.05.018
31. Tanaka N, McCalley D V. Core-shell, ultra-small particles, monoliths, and other support materials in high-performance liquid chromatography. *Anal Chem*. 2016;88(1):279-298. https://doi.org/10.1021/acs.analchem.5b04093
32. Leśko M, Samuelsson J, Åsberg D, Kaczmarski K, Fornstedt T. Evaluating the advantages of higher heat conductivity in a recently developed type of core-shell diamond stationary phase particle in UHPLC. *J Chromatogr A*. 2020;1625:461076. https://doi.org/10.1016/j.chroma.2020.461076
33. Wouters S, Dores-Sousa JL, Liu Y, Pohl CA, Eeltink S. Ultra-high-pressure ion chromatography with suppressed conductivity detection at 70 MPa using columns packed with 2.5 μm anion-exchange particles. *Anal Chem*. 2019;91(21):13824-13830. https://doi.org/10.1021/acs.analchem.9b03283
34. Gritti F, Gilar M. Impact of frit dispersion on gradient performance in high-throughput liquid chromatography. *J Chromatogr A*. 2019;1591:110-119. https://doi.org/10.1016/j.chroma.2019.01.021
35. Zelenyánszki D, Lambert N, Gritti F, Felinger A. The effect of column packing procedure on column end efficiency and on bed heterogeneity – Experiments with flow-reversal. *J Chromatogr A*. 2019;1603:412-416. https://doi.org/10.1016/j.chroma.2019.05.040
36. Zelenyánszki D, Mester A, Felinger A. Flow-reversal experiments with macromolecules to measure column end efficiency and bed heterogeneity. *Chromatographia*. 2019;82(9):1303-1309. https://doi.org/10.1007/s10337-019-03759-0
37. De Vos J, Baron G V., Wirth MJ, Terryn H, Kaal ER, Eeltink S. Evaluation of particle and bed integrity of aqueous size-exclusion columns packed with sub-2 μm particles operated at high pressure. *J Chromatogr A*. 2020;1621:461064. https://doi.org/10.1016/j.chroma.2020.461064
38. Desmet G, Broeckhoven K. Extra-column band broadening effects in contemporary liquid chromatography: Causes and solutions. *TrAC Trends Anal Chem*. 2019;119:115619. https://doi.org/10.1016/j.trac.2019.115619
39. Zhou Z, De Pra M, Steiner F, Desmet G, Sebastiaan E. Assessing effects of ultra-high-pressure liquid chromatography instrument configuration on dispersion, system pressure, and retention. *J Chromatogr A*. 2020; In Press:461660. https://doi.org/10.1016/j.chroma.2020.461660
40. Vanderlinden K, Broeckhoven K, Vanderheyden Y, Desmet G. Effect of pre- and post-column band broadening on the performance of high-speed chromatography columns under isocratic and gradient conditions. *J Chromatogr A*. 2016;1442:73-82. https://doi.org/10.1016/j.chroma.2016.03.016
41. Kaplitz AS, Kresge GA, Selover B, et al. High-throughput and ultra-fast liquid chromatography. *Anal Chem*. 2020;92(1):67-84. https://doi.org/10.1021/acs.analchem.9b04713
42. Gilar M, McDonald TS, Gritti F. Impact of instrument and column parameters on high-throughput liquid chromatography performance. *J Chromatogr A*. 2017;1523:215-223. https://doi.org/10.1016/j.chroma.2017.07.035
43. Dolan JW. How does it work? Part I: pumps. *LC-GC North Am*. 2016;34(5):324-329.
44. Shoykhet K, Broeckhoven K, Dong MW. Modern HPLC pumps: perspectives, principles, and practices. *LC-GC North Am*. 2019;37(6):374-384.
45. Pauw R De, Degreef B, Ritchie H, Eeltink S, Desmet G, Broeckhoven K. Extending the limits of operating pressure of narrow-bore column liquid chromatography instrumentation. *J Chromatogr A*. 2014;1347:56-62. https://doi.org/10.1016/j.chroma.2014.04.056
46. De Pauw R, Swier T, Degreef B, Desmet G, Broeckhoven K. On the feasibility to conduct gradient liquid chromatography separations in

narrow-bore columns at pressures up to 2000 bar. *J Chromatogr A*. 2016;1473:48-55. https://doi.org/10.1016/j.chroma.2016.10.008
47. Grinias KM, Godinho JM, Franklin EG, Stobaugh JT, Jorgenson JW. Development of a 45kpsi ultrahigh pressure liquid chromatography instrument for gradient separations of peptides using long microcapillary columns and sub-2μm particles. *J Chromatogr A*. 2016;1469:60-67. https://doi.org/10.1016/j.chroma.2016.09.053
48. Sorensen MJ, Anderson BG, Kennedy RT. Liquid chromatography above 20000 PSI. *TrAC - Trends Anal Chem*. 2020;124:115810. https://doi.org/10.1016/j.trac.2020.115810
49. Sorensen MJ, Miller KE, Jorgenson JW, Kennedy RT. Ultrahigh-performance capillary liquid chromatography-mass spectrometry at 35 kpsi for separation of lipids. *J Chromatogr A*. 2020;1611:460575. https://doi.org/10.1016/j.chroma.2019.460575
50. Miller KE, Jorgenson JW. Comparison of microcapillary column length and inner diameter investigated with gradient analysis of lipids by ultrahigh-pressure liquid chromatography-mass spectrometry. *J Sep Sci*. 2020. In Press. https://doi.org/10.1002/jssc.202000545
51. Broeckhoven K, Billen J, Verstraeten M, et al. Towards a solution for viscous heating in ultra-high pressure liquid chromatography using intermediate cooling. *J Chromatogr A*. 2010;1217(13):2022-2031. https://doi.org/10.1016/j.chroma.2010.01.072
52. Gritti F, Wahab MF, Farooq Wahab M, Wahab MF. Understanding the science behind packing high-efficiency columns and capillaries: Facts, fundamentals, challenges, and future directions. *LC-GC North Am*. 2018;36(2):82-98.
53. Broeckhoven K, Verstraeten M, Choikhet K, Dittmann M, Witt K, Desmet G. Kinetic performance limits of constant pressure versus constant flow rate gradient elution separations. Part I: Theory. *J Chromatogr A*. 2011;1218(8):1153-1169. https://doi.org/10.1016/j.chroma.2010.12.086
54. Verstraeten M, Broeckhoven K, Dittmann M, Choikhet K, Witt K, Desmet G. Kinetic performance limits of constant pressure versus constant flow rate gradient elution separations. Part II: Experimental. *J Chromatogr A*. 2011;1218(8):1170-1184. https://doi.org/10.1016/j.chroma.2010.12.087
55. Gritti F, Stankovich JJ, Guiochon G. Potential advantage of constant pressure versus constant flow gradient chromatography for the analysis of small molecules. *J Chromatogr A*. 2012;1263:51-60. https://doi.org/10.1016/j.chroma.2012.09.004
56. Verstraeten M, Witt K, Choikhet K, Desmet G. Maximizing Robustness and Throughput in Liquid Chromatography by Using Pressure-Controlled Operation. *LC-GC North Am*. 2012;30(12):0-6.
57. Verstraeten M, Broeckhoven K, Lynen F, et al. Comparison of the quantitative performance of constant pressure versus constant flow rate gradient elution separations using concentration-sensitive detectors. *J Chromatogr A*. 2012;1232:65-76. https://doi.org/10.1016/j.chroma.2011.10.019
58. Verstraeten M, Broeckhoven K, Lynen F, et al. Quantification aspects of constant pressure (ultra) high pressure liquid chromatography using mass-sensitive detectors with a nebulizing interface. *J Chromatogr A*. 2013;1274:118-128. https://doi.org/10.1016/j.chroma.2012.12.013
59. Gritti F, Guiochon G. Theoretical comparison of the performance of gradient elution chromatography at constant pressure and constant flow rate. *J Chromatogr A*. 2012;1253:71-82. https://doi.org/10.1016/j.chroma.2012.06.092
60. Fekete S, Fekete J, Guillarme D. Estimation of the effects of longitudinal temperature gradients caused by frictional heating on the solute retention using fully porous and superficially porous sub-2μm materials. *J Chromatogr A*. 2014;1359:124-130. https://doi.org/10.1016/j.chroma.2014.07.030
61. Dolan JW. How does it work? Part III: Autosamplers. *LC-GC North Am*. 2016;34(7):472-478.
62. Paul C, Steiner F, Dong MW. HPLC autosamplers: perspectives, principles, and practices. *LCGC North Am*. 2019;37(8): 514-529.
63. Terada H, Koterasawa K, Kihara T. Increased analysis throughput by overlapped injection using the SIL-40 series autosampler. Shimadzu Technical Report. 2019:C190-E235.
64. Dong MW. New HPLC systems and related products introduced in 2017-2018: A brief review. *LC-GC North Am*. 2018;36(4):256-265.
65. Schneider S, Metzlaff M. Ultrafast analysis of food preservatives using automated column regeneration and dual-needle injection. Agilent Technologies Application Note. 2015:5991-6150E.
66. Schuhn B. Minimizing sample carryover using the multiwash function of the agilent 1290 infinity II multisampler. Agilent Technologies Application Note. 2015:5991-6246E.
67. Grosse S, Pra M De, Steiner F. Doubling the throughput of long chromatographic methods by using a novel Dual LC workflow. Thermo Fisher Scientific Application Note. 2018:72601.
68. Grosse S, Pra M De, Steiner F. Simultaneous determination of water- and fat-soluble vitamins in tablets and energy drinks by using a novel Vanquish Flex Duo system for Dual LC. Thermo Fisher Scientific Application Note. 2018:72592.
69. Grübner M, Paul C. Simultaneous high-performance and ultra-high-performance liquid chromatographic analysis of acetaminophen impurities using a single instrument. Thermo Fish Sci Appl Note. 2018;(72593).
70. Grinias JP, Wong J-MT, Kennedy RT. Repeatability of gradient ultra-high pressure liquid chromatography–tandem mass spectrometry methods in instrument-controlled thermal environments. *J Chromatogr A*. 2016;1461:42-50. https://doi.org/10.1016/j.chroma.2016.07.043
71. Kresge GA, Wong J-MT, De Pra M, Steiner F, Grinias JP. Using superficially porous particles and ultrahigh pressure liquid chromatography in pharmacopeial monograph modernization of common analgesics. *Chromatographia*. 2019;82(1):465-475. https://doi.org/10.1007/s10337-018-3593-2
72. Gritti F, Guiochon G. Optimization of the thermal environment of columns packed with very fine particles. *J Chromatogr A*. 2009;1216(9):1353-1362. https://doi.org/10.1016/j.chroma.2008.12.072
73. Grinias JP, Keil DS, Jorgenson JW. Observation of enhanced heat dissipation in columns packed with superficially porous particles. *J Chromatogr A*. 2014;1371:261-264. https://doi.org/10.1016/j.chroma.2014.10.075
74. Lambert N, Felinger A. The effect of the frictional heat on retention and efficiency in thermostated or insulated chromatographic columns packed with sub-2-μm particles. *J Chromatogr A*. 2018;1565:89-95. https://doi.org/10.1016/j.chroma.2018.06.038
75. Makarov AA, Mann BF, Regalado EL, et al. Visualizing and studying frictional heating effects in reversed-phase liquid chromatography using infrared thermal imaging. *Anal Chim Acta*. 2018;1018:1-6. https://doi.org/10.1016/j.aca.2018.02.061
76. Vera CM, Samuelsson J, Fornstedt T, Dennis GR, Shalliker RA. Protocol for the visualisation of axial temperature gradients in ultra high performance liquid chromatography using infrared cameras. *Microchem J*. 2018;141:141-147. https://doi.org/10.1016/j.microc.2018.05.004
77. Vera CM, Samuelsson J, Fornstedt T, Dennis GR, Shalliker RA. Visualisation of axial temperature gradients and heat transfer process of different solvent compositions in ultra high performance liquid chromatography using thermography. *Microchem J*. 2019;145:927-935. https://doi.org/10.1016/j.microc.2018.11.037
78. Gritti F, Gilar M, Jarrell JA. Achieving quasi-adiabatic thermal environment to maximize resolution power in very high-pressure liquid chromatography: Theory, models, and experiments. *J Chromatogr A*. 2016;1444:86-98. https://doi.org/10.1016/j.chroma.2016.03.070

79. Gritti F, Gilar M, Jarrell JA. Quasi-adiabatic vacuum-based column housing for very high-pressure liquid chromatography. *J Chromatogr A*. 2016;1456:226-234. https://doi.org/10.1016/j.chroma.2016.06.029
80. Gritti F. Designing Vacuum-Jacketed User-Friendly Columns for Maximum Resolution Under Extreme UHPLC and SFC Conditions 10 -5. *LC-GC North Am*. 2018;36(6):18-24.
81. Deridder S, Smits W, Broeckhoven K, Desmet G. A multiscale modelling study on the sense and nonsense of thermal conductivity enhancement of liquid chromatography packings and other potential solutions for viscous heating effects. *J Chromatogr A*. 2020;1620:461022. https://doi.org/10.1016/j.chroma.2020.461022
82. Akita S, Watanabe K. New analytical intelligence concept - support for automating analytical operations. Shimadzu Technical Report. 2019:TR C190-E2.
83. Gomi T, Vecchietti D. Use of Solvent Delivery Unit Equipped with Auto-Diagnostics and Auto-Recovery Functions to Enhance Lab Productivity. Shimadzu Corp. 2019;(TR C190-E225).
84. Saki Y, Vecchietti D. Maximizing Analytical Efficiency with Real-Time Measurement of Mobile Phase Consumption. Shimadzu Corp. 2019;(TR C190-E226).
85. Köhler D, Greco G, Moore D. Ensuring robust sequences through automatic continuous management of HPLC mobile phases and waste. Thermo Fisher Scientific. 2019:SP73233-EN 1219C.
86. Christ B, Schloderer R. Volume measurement of a liquid, method and device. 2013;(US 2013/0276524 A1).
87. Hormann K, Franz H. System health checks - a novel software tool to prevent unplanned HPLC system downtime. Thermo Fisher Scientific. 2020:PS-73375.
88. Dolan JW. How does it work? Part IV: Ultraviolet detectors. *LC-GC North Am*. 2016;34(8):534-539.
89. Dong MW, Wysocki J. Ultraviolet Detectors: Perspectives, Principles, and Practices. *LC-GC North Am*. 2019;37(10):750-759.
90. Kraiczek KG, Rozing GP, Zengerle R. Relation between chromatographic resolution and signal-to-noise ratio in spectrophotometric HPLC detection. *Anal Chem*. 2013;85(10):4829-4835. https://doi.org/10.1021/ac4004387
91. Kadjo AF, Dasgupta PK, Shelor CP. Optimum cell pathlength or volume for absorbance detection in liquid chromatography: transforming longer cell results to virtual shorter cells. *Anal Chem*. 2020;92(9):6391-6400. https://doi.org/10.1021/acs.analchem.9b05464
92. Technologies A. 10 x more sensitivity with the Agilent 1290 /1260 Infinity Diode Array Detector compared to Agilent 1200 Series UV Detectors. Agilent Technical Note. 2010:TN 5990-5326EN.
93. Enhancement of sensitivity of photodiode array detector SPD-M30A by new HS capillary flow cell. Shimadzu Appl Data Sheet. 2013:AD-0064.
94. Manka A, Franz H. Boosting trace detection performance with the Vanquish diode array detector and high-sensitivity LightPipe flow Cell. Thermo Fisher Scientific. 2016:TN-71674.
95. Dasgupta PK, Shelor CP, Kadjo AF, Kraiczek KG. Flow-cell-induced dispersion in flow-through absorbance detection systems: true column effluent peak variance. *Anal Chem*. 2018;90(3):2063-2069. https://doi.org/10.1021/acs.analchem.7b04248
96. Vanderlinden K, Desmet G, Broeckhoven K. Measurement of the band broadening of UV detectors used in ultra-high performance liquid chromatography using an on-tubing fluorescence detector. *Chromatographia*. 2019;82(1):489-498. https://doi.org/10.1007/s10337-018-3622-1
97. Wahab MF, Dasgupta PK, Kadjo AF, Armstrong DW. Sampling frequency, response times and embedded signal filtration in fast, high efficiency liquid chromatography: A tutorial. *Anal Chim Acta*. 2016;907:31-44. https://doi.org/10.1016/j.aca.2015.11.043
98. Arase S, Horie K, Kato T, et al. Intelligent peak deconvolution through in-depth study of the data matrix from liquid chromatography coupled with a photo-diode array detector applied to pharmaceutical analysis. *J Chromatogr A*. 2016;1469:35-47. https://doi.org/10.1016/j.chroma.2016.09.037
99. Cook DW, Rutan SC, Venkatramani CJ, Stoll DR. Peak purity in liquid chromatography, part 2: Potential of curve resolution techniques. *LC-GC North Am*. 2018;36(4):248-255.
100. Hellinghausen G, Farooq Wahab M, Armstrong DW. Improving visualization of trace components for quantification using a power law based integration approach. *J Chromatogr A*. 2018;1574:1-8. https://doi.org/10.1016/j.chroma.2018.09.002
101. Wahab MF, Gritti F, O'Haver TC, Hellinghausen G, Armstrong DW. Power Law Approach as a Convenient Protocol for Improving Peak Shapes and Recovering Areas from Partially Resolved Peaks. *Chromatographia*. 2019;82(1):211-220. https://doi.org/10.1007/s10337-018-3607-0
102. Wahab MF, Berthod A, Armstrong DW. Extending the power transform approach for recovering areas of overlapping peaks. *J Sep Sci*. 2019;42(24):3604-3610. https://doi.org/10.1002/jssc.201900799
103. Wahab MF, O'Haver TC, Gritti F, Hellinghausen G, Armstrong DW. Increasing chromatographic resolution of analytical signals using derivative enhancement approach. *Talanta*. 2019;192:492-499. https://doi.org/10.1016/j.talanta.2018.09.048
104. Zhang K, Kurita KL, Venkatramani C, Russell D. Seeking universal detectors for analytical characterizations. *J Pharm Biomed Anal*. 2019;162:192-204. https://doi.org/10.1016/j.jpba.2018.09.029
105. Schilling K, Holzgrabe U. Recent applications of the Charged Aerosol Detector for liquid chromatography in drug quality control. *J Chromatogr A*. 2020;1619:460911. https://doi.org/10.1016/j.chroma.2020.460911
106. Fibigr J, Šatínský D, Solich P. A UHPLC method for the rapid separation and quantification of phytosterols using tandem UV/Charged aerosol detection – A comparison of both detection techniques. *J Pharm Biomed Anal*. 2017;140:274-280. https://doi.org/10.1016/j.jpba.2017.03.057
107. Schilling K, Pawellek R, Lovejoy K, Muellner T, Holzgrabe U. Influence of charged aerosol detector instrument settings on the ultra-high-performance liquid chromatography analysis of fatty acids in polysorbate 80. *J Chromatogr A*. 2018;1576:58-66. https://doi.org/10.1016/j.chroma.2018.09.031
108. López-Ruiz R, Romero-González R, Garrido Frenich A. Ultrahigh-pressure liquid chromatography-mass spectrometry: An overview of the last decade. *TrAC - Trends Anal Chem*. 2019;118:170-181. https://doi.org/10.1016/j.trac.2019.05.044
109. Kaufmann A. Combining UHPLC and high-resolution MS: A viable approach for the analysis of complex samples? *TrAC - Trends Anal Chem*. 2014;63:113-128. https://doi.org/10.1016/j.trac.2014.06.025
110. Spaggiari D, Fekete S, Eugster PJ, et al. Contribution of various types of liquid chromatography – mass spectrometry instruments to band broadening in fast analysis. *J Chromatogr A*. 2013;1310:45-55. https://doi.org/10.1016/j.chroma.2013.08.001
111. Hopfgartner G. Can MS fully exploit the benefits of fast chromatography? *Bioanalysis*. 2011;3(2):121-123. https://doi.org/10.4155/bio.10.191
112. Fenaille F, Barbier Saint-Hilaire P, Rousseau K, Junot C. Data acquisition workflows in liquid chromatography coupled to high resolution mass spectrometry-based metabolomics: Where do we stand? *J Chromatogr A*. 2017;1526:1-12. https://doi.org/10.1016/j.chroma.2017.10.043
113. Eliuk S, Makarov A. Evolution of Orbitrap Mass Spectrometry Instrumentation. *Annu Rev Anal Chem*. 2015;8(1):61-80. https://doi.org/10.1146/annurev-anchem-071114-040325

114. Kaufmann A. Analytical performance of the various acquisition modes in Orbitrap MS and MS/MS. *J Mass Spectrom*. 2018;53(8):725-738. https://doi.org/10.1002/jms.4007
115. Kempa EE, Hollywood KA, Smith CA, Barran PE. High throughput screening of complex biological samples with mass spectrometry-from bulk measurements to single cell analysis. *Analyst*. 2019;144(3):872-891. https://doi.org/10.1039/c8an01448e
116. Pu F, Elsen NL, Williams JD. Emerging chromatography-free high-throughput mass spectrometry technologies for generating hits and leads. *ACS Med Chem Lett*. 2020;(11):2108-2113. https://doi.org/10.1021/acsmedchemlett.0c00314
117. Gosetti F, Mazzucco E, Zampieri D, Gennaro MC. Signal suppression/enhancement in high-performance liquid chromatography tandem mass spectrometry. *J Chromatogr A*. 2010;1217(25):3929-3937. https://doi.org/10.1016/j.chroma.2009.11.060
118. Marchetti N, Fairchild JN, Guiochon G. Comprehensive off-line, two-dimensional liquid chromatography. Application to the separation of peptide digests. *Anal Chem*. 2008;80(8):2756-2767. https://doi.org/10.1021/ac7022662
119. Horváth K, Fairchild J, Guiochon G. Optimization strategies for off-line two-dimensional liquid chromatography. *J Chromatogr A*. 2009;1216:2511-2518. https://doi.org/10.1016/j.chroma.2009.01.064
120. Guiochon G, Marchetti N, Mriziq K, Shalliker RA. Implementations of two-dimensional liquid chromatography. *J Chromatogr A*. 2008;1189(1-2):109-168. https://doi.org/10.1016/j.chroma.2008.01.086
121. Johnson EL, Gloor R, Majors RE. Coupled column chromatography employing exclusion and a reversed phase: A potential general approach to sequential analysis. *J Chromatogr A*. 1978;149:571-585.
122. Zhang K, Li Y, Tsang M, Chetwyn NP. Analysis of pharmaceutical impurities using multi-heartcutting 2D LC coupled with UV-charged aerosol MS detection. *J Sep Sci*. 2013;36:2986-2992. https://doi.org/10.1002/jssc.201300493
123. Groskreutz SR, Swenson MM, Secor LB, Stoll DR. Selective comprehensive multi-dimensional separation for resolution enhancement in high performance liquid chromatography. Part I: Principles and instrumentation. *J Chromatogr A*. 2012;1228:31-40. https://doi.org/10.1016/j.chroma.2011.06.035
124. Groskreutz SR, Swenson MM, Secor LB, Stoll DR. Selective comprehensive multidimensional separation for resolution enhancement in high performance liquid chromatography. Part II: Applications. *J Chromatogr A*. 2012;1228:41-50. https://doi.org/10.1016/j.chroma.2011.06.038
125. Larson ED, Groskreutz SR, Harmes DC, et al. Development of selective comprehensive two-dimensional liquid chromatography with parallel first-dimension sampling and second-dimension separation — application to the quantitative analysis of furanocoumarins in apiaceous vegetables. *Anal Bioanal Chem*. 2013;405:4639-4653. https://doi.org/10.1007/s00216-013-6758-8
126. Petersson P, Haselmann K, Buckenmaier S. Multiple heart-cutting two dimensional liquid chromatography mass spectrometry: Towards real time determination of related impurities of biopharmaceuticals in salt based separation methods. *J Chromatogr A*. 2016;1468:95-101. https://doi.org/10.1016/j.chroma.2016.09.023
127. De Vos J, Eeltink S, Desmet G. Peak refocusing using subsequent retentive trapping and strong eluent remobilization in liquid chromatography: A theoretical optimization study. *J Chromatogr A*. 2015;1381:74-86. https://doi.org/10.1016/j.chroma.2014.12.082
128. De Vos J, Desmet G, Eeltink S. A generic approach to post-column refocusing in liquid chromatography. *J Chromatogr A*. 2014;1360:164-171. https://doi.org/10.1016/j.chroma.2014.07.072
129. De Vos J, Desmet G, Eeltink S. Enhancing detection sensitivity in gradient liquid chromatography via post-column refocusing and strong-solvent remobilization. *J Chromatogr A*. 2016;1455:86-92. https://doi.org/10.1016/j.chroma.2016.05.046
130. Eghbali H, Sandra K, Tienpont B, Eeltink S, Sandra P, Desmet G. Exploring the possibilities of cryogenic cooling in liquid chromatography for biological applications: A proof of principle. *Anal Chem*. 2012;84(4):2031-2037. https://doi.org/10.1021/ac203252u
131. Verstraeten M, Pursch M, Eckerle P, Luong J, Desmet G. Thermal modulation for multidimensional liquid chromatography separations using low-thermal-mass liquid chromatography (LC). *Anal Chem*. 2011;83(18):7053-7060. https://doi.org/10.1021/ac201207t
132. Rerick MT, Groskreutz SR, Weber SG. Multiplicative on-column solute focusing using spatially dependent temperature programming for capillary HPLC. *Anal Chem*. 2019;91:2854–2860. https://doi.org/10.1021/acs.analchem.8b04826
133. Stoll DR, Carr PW. Two-dimensional liquid chromatography: A state of the art tutorial. *Anal Chem*. 2016;89(1):519-531. https://doi.org/10.1021/acs.analchem.6b03506
134. Stoll DR, Shoykhet K, Petersson P, Buckenmaier S. Active solvent modulation: A valve-based approach to improve separation compatibility in two-dimensional liquid chromatography. *Anal Chem*. 2017;89:9260−9267. https://doi.org/10.1021/acs.analchem.7b02046
135. Pursch M, Wegener A, Buckenmaier S. Evaluation of active solvent modulation to enhance two-dimensional liquid chromatography for target analysis in polymeric matrices. *J Chromatogr A*. 2018;1562:78-86. https://doi.org/10.1016/j.chroma.2018.05.059
136. Pirok BWJ, Gargano AFG, Schoenmakers PJ. Optimizing separations in online comprehensive two-dimensional liquid chromatography. *J Sep Sci*. 2018;41:68-98. https://doi.org/10.1002/jssc.201700863
137. Leonhardt J, Teutenberg T, Tuerk J, Schlüsener MP, Ternes TA, Schmidt TC. A comparison of one-dimensional and microscale two-dimensional liquid chromatographic approaches coupled to high resolution mass spectrometry for the analysis of complex samples. *Anal Methods*. 2015;7:7697-7706. https://doi.org/10.1039/c5ay01143d
138. Tian H, Xu J, Xu Y, Guan Y. Multidimensional liquid chromatography system with an innovative solvent evaporation interface. *J Chromatogr A*. 2006;1137:42-48. https://doi.org/10.1016/j.chroma.2006.10.005
139. Tian H, Xu J, Guan Y. Comprehensive two-dimensional liquid chromatography (NPLC x RPLC) with vacuum- evaporation interface. *J Sep Sci*. 2008;31:1677-1685. https://doi.org/10.1002/jssc.200700559
140. Fornells E, Barnett B, Bailey M, Hilder EF, Shellie RA, Breadmore MC. Evaporative membrane modulation for comprehensive two- dimensional liquid chromatography. *Anal Chim Acta*. 2018;1000:303-309. https://doi.org/10.1016/j.aca.2017.11.053
141. Gargano AFG, Duffin M, Navarro P, Schoenmakers PJ. Reducing dilution and analysis time in online comprehensive two-dimensional liquid chromatography by active modulation. *Anal Chem*. 2016;88(3):1785-1793. https://doi.org/10.1021/acs.analchem.5b04051
142. Karongo R, Ikegami T, Stoll DR, Lämmerhofer M. A selective comprehensive reversed-phase × reversed-phase 2D-liquid chromatography approach with multiple complementary detectors as advanced generic method for the quality control of synthetic and therapeutic peptides. *J Chromatogr A*. 2020;1627:461430. https://doi.org/10.1016/j.chroma.2020.461430
143. Stoll DR, Harmes DC, Staples GO, et al. Development of comprehensive online two-dimensional liquid chromatography/mass spectrometry using hydrophilic interaction and reversed-phase separations for rapid and deep profiling of therapeutic antibodies. *Anal Chem*. 2018;90:5923−5929. https://doi.org/10.1021/acs.analchem.8b00776
144. Yang P, Sattler W, Gao W, et al. Two-dimensional liquid chromatography with active solvent modulation for studying monomer

incorporation in copolymer dispersants. 2019;(June):1-11. https://doi.org/10.1002/jssc.201900283
145. De Vos J, Dams M, Broeckhoven K, Desmet G, Horstkotte B, Eeltink S. Prototyping of a microfluidic modulator chip and its application in heart-cut strong-cation-exchange - reversed-phase liquid chromatography coupled to nano-electrospray mass spectrometry for targeted proteomics. *Anal Chem*. 2020;92(3):2388-2392. https://doi.org/10.1021/acs.analchem.9b05141
146. Wei Z, Zhang X, Zhao X, Jiao Y, Huang Y, Liu Z. Construction of a microfluidic platform integrating online protein fractionation, denaturation, digestion, and peptide enrichment. *Talanta*. 2020. https://doi.org/10.1016/j.talanta.2020.121810
147. Yin H, Killeen K, Brennen R, Sobek D, Werlich M, Van De Goor T. Microfluidic chip for peptide analysis with an integrated HPLC column, sample enrichment column, and nanoelectrospray tip. *Anal Chem*. 2005;77(2):527-533. https://doi.org/10.1021/ac049068d
148. Piendl SK, Geissler D, Weigelt L, Belder D. Multiple heart-cutting two-dimensional chip-HPLC combined with deep-UV fluorescence and mass spectrometric detection. *Anal Chem*. 2020;93:3795−3803. https://doi.org/10.1021/acs.analchem.9b05206
149. Chen Y, Li J, Schmitz OJ. Development of an at-column dilution modulator for flexible and precise control of dilution factors to overcome mobile phase incompatibility in comprehensive two-dimensional liquid chromatography. *Anal Chem*. 2019;91(15):10251-10257. https://doi.org/10.1021/acs.analchem.9b02391
150. Chen Y, Montero L, Luo J, Li J, Schmitz OJ. Application of the new at-column dilution (ACD) modulator for the two-dimensional RP×HILIC analysis of Buddleja davidii. *Anal Bioanal Chem*. 2020;412(7):1483-1495. https://doi.org/10.1007/s00216-020-02392-3
151. Chen Y, Montero L, Schmitz OJ. Advance in on-line two-dimensional liquid chromatography modulation technology. *TrAC - Trends Anal Chem*. 2019;120:115647. https://doi.org/10.1016/j.trac.2019.115647
152. Wouters B, Davydova E, Wouters S, Vivo-Truyols G, Schoenmakers PJ, Eeltink S. Towards ultra-high peak capacities and peak-production rates using spatial three-dimensional liquid chromatography. *Lab Chip*. 2015;15(October):4415-4422. https://doi.org/10.1039/c5lc01169h
153. Wouters B, De Vos J, Desmet G, Terryn H, Schoenmakers PJ, Eeltink S. Design of a microfluidic device for comprehensive spatial two-dimensional liquid chromatography. *J Sep Sci*. 2015;38:1123-1129.
154. De Vos J, Eeltink S. Prototyping of novel microfluidic chips for comprehensive two- and three-dimension liquid chromatographic separations. In: 37th International Symposium on High Performace Liquid Phase Separations and Related Techniques; 2018.
155. Adamopoulou T, Deridder S, Nawada SH, Desmet G, Schoenmakers PJ. Creating devices for multidimensional separations based on computational insights. In: 37th International Symposium on High Performace Liquid Phase Separations and Related Techniques; 2018.
156. Adamopoulou T, Deridder S, Desmet G, Schoenmakers PJ. Two-dimensional insertable separation tool (TWIST) for flow confinement in spatial separations. *J Chromatogr A*. 2018;1577:120-123. https://doi.org/10.1016/j.chroma.2018.09.054
157. Themelis T, De Vos J, Dores-Sousa JL, van Assche T, Eeltink S. Engineering solutions for flow control in microfluidic devices for spatial multi-dimensional liquid chromatography. *Sensors Actuators, B Chem*. 2020;320(May 2020). https://doi.org/10.1016/j.snb.2020.128388
158. Adamopoulou T, Nawada S, Deridder S, Wouters B, Desmet G, Schoenmakers PJ. Experimental and numerical study of band-broadening effects associated with analyte transfer in microfluidic devices for spatial two-dimensional liquid chromatography created by additive manufacturing. *J Chromatogr A*. 2019;1598:77-84. https://doi.org/10.1016/j.chroma.2019.03.041
159. Adamopoulou T, Deridder S, Bos TS, Nawada S, Desmet G, Schoenmakers PJ. Optimizing design and employing permeability differences to achieve flow confinement in devices for spatial multidimensional liquid chromatography. *J Chromatogr A*. 2020;1612:460665. https://doi.org/10.1016/j.chroma.2019.460665
160. Komendová M, Nawada S, Metelka R, Schoenmakers PJ, Urban J. Multichannel separation device with parallel electrochemical detection. *J Chromatogr A*. 2020;1610. https://doi.org/10.1016/j.chroma.2019.460537
161. Themelis T, Amini A, De Vos J, Eeltink S. Towards spatial comprehensive three-dimensional liquid chromatographic separations: a tutorial review. *Anal Chim Acta*. 2020;(Accepted). https://doi.org/10.1016/j.aca.2020.12.032
162. Mccalley DV. Managing the column equilibration time in hydrophilic interaction chromatography. *J Chromatogr A*. 2020;1612:460655. https://doi.org/10.1016/j.chroma.2019.460655
163. Berthelette KD, Walter TH, Gilar M, Gritti F, Macdonald TS, Soares M. Evaluating MISER chromatography as a tool for characterizing HILIC column equilibration. *J Chromatogr A*. 2020;1619:460931. https://doi.org/10.1016/j.chroma.2020.460931
164. Welch CJ, Gong X, Schafer W, et al. MISER chromatography (multiple injections in a single experimental run): the chromatogram is the graph. *Tetrahedron: Asymmetry*. 2010;21(13-14):1674-1681. https://doi.org/10.1016/j.tetasy.2010.05.029
165. Carillo S, Martín SM, Bones J. High-throughput peptide mapping of trastuzumab using a tandem LC-MS workflow. Thermo Fish Sci Appl Note. 2020;(73784).
166. Sorensen MJ, Anderson BG, Kennedy RT. Trends in Analytical Chemistry Liquid chromatography above 20, 000 PSI. *Trends Anal Chem*. 2020;124:115810. https://doi.org/10.1016/j.trac.2020.115810
167. Stoll DR. Chapter 7 - Introduction to two-dimensional liquid chromatography—theory and practice. In: Holčapek M, Byrdwell WC, eds. *Handbook of Advanced Chromatography/Mass Spectrometry Techniques*. AOCS Press; 2017:227-286. https://doi.org/10.1016/B978-0-12-811732-3.00007-8
168. Regalado EL, Haidar Ahmad IA, Bennett R, et al. The emergence of universal chromatographic methods in the research and development of new drug substances. *Acc Chem Res*. 2019;52:1990–2002. https://doi.org/10.1021/acs.accounts.9b00068
169. Multi-Dimensional Separations. http://www.multidlc.org/.
170. Wang H, Lhotka HR, Bennett R, et al. Introducing online multicolumn two-dimensional liquid chromatography screening for facile selection of stationary and mobile phase conditions in both dimensions. *J Chromatogr A*. 2020;1622:460895. https://doi.org/10.1016/j.chroma.2020.460895
171. Venkatramani CJ, Al-sayah M, Li G, et al. Simultaneous achiral-chiral analysis of pharmaceutical compounds using two-dimensional reversed phase liquid chromatography-supercritical fl uid chromatography. *Talanta*. 2016;148:548-555. https://doi.org/10.1016/j.talanta.2015.10.054
172. Makey DM, Shchurik V, Wang H, et al. Mapping the separation landscape in two-dimensional liquid chromatography : Blueprints for efficient analysis and purification of pharmaceuticals enabled by computer-assisted modeling. *Anal Chem*. 2020. https://doi.org/10.1021/acs.analchem.0c03680
173. Stephan S, Jakob C, Hippler J, Schmitz OJ. A novel four-dimensional analytical approach for analysis of complex samples. *Anal Bioanal Chem*. 2016;408(14):3751-3759. https://doi.org/10.1007/s00216-016-9460-9
174. Stephan S, Hippler J, Köhler T, Deeb AA, Schmidt TC, Schmitz OJ. Contaminant screening of wastewater with HPLC-IM-qTOF-MS and LC + LC-IM-qTOF-MS using a CCS database. *Anal Bioanal Chem*. 2016;408:6545–6555. https://doi.org/10.1007/s00216-016-9820-5
175. Ehkirch A, Goyon A, Hernandez-alba O, et al. A novel online four-dimensional SEC × SEC-IM × MS methodology for characterization of monoclonal antibody size variants. *Anal Chem*.

2018;90:13929−13937. https://doi.org/10.1021/acs.analchem.8b03333
176. Ehkirch A, Atri VD, Rouviere F, et al. An online four-dimensional HIC × SEC-IM × MS methodology for proof-of-concept characterization of antibody drug conjugates. *Anal Chem*. 2018;90:1578−1586. https://doi.org/10.1021/acs.analchem.7b02110
177. Venter P, Muller M, Vestner J, et al. Comprehensive three-dimensional LC × LC × ion mobility spectrometry separation combined with high-resolution MS for the analysis of complex samples. *Anal Chem*. 2018;90:11643−11650. https://doi.org/10.1021/acs.analchem.8b03234
178. Gstöttner C, Klemm D, Haberger M, et al. Fast and automated characterization of antibody variants with 4D HPLC/MS. *Anal Chem*. 2018;90(3):2119–2125. https://doi.org/10.1021/acs.analchem.7b04372
179. Camperi J, Dai L, Guillarme D, Stella C. Fast and automated characterization of monoclonal antibody minor variants from cell cultures by combined protein – a and multidimensional LC/MS methodologies. *Anal Chem*. 2020;92(12):8506–8513. https://doi.org/10.1021/acs.analchem.0c01250
180. Camperi J, Dai L, Guillarme D, Stella C. Development of a 3D-LC/MS workflow for fast, automated, and effective characterization of glycosylation patterns of biotherapeutic products. *Anal Chem*. 2020;92:4357–4363. https://doi.org/10.1021/acs.analchem.9b05193
181. Camperi J, Guillarme D, Stella C. Targeted bottom-up characterization of recombinant monoclonal antibodies by multidimensional LC/MS. *Anal Chem*. 2020;92:13420–13426. https://doi.org/10.1021/acs.analchem.0c02780
182. Pirok BWJ, Pous-Torres S, Ortiz-Bolsico C, Vivó-Truyols G, Schoenmakers PJ. Program for the interpretive optimization of two-dimensional resolution. *J Chromatogr A*. 2016;1450:29-37. https://doi.org/10.1016/j.chroma.2016.04.061

**How to cite this article:** De Vos J, Stoll D, Buckenmaier S, Eeltink S, Grinias JP. Advances in ultra-high-pressure and multi-dimensional liquid chromatography instrumentation and workflows. *Anal Sci Adv*. 2021;2:171–192. https://doi.org/10.1002/ansa.202100007